

## REVIEW ARTICLE

# The recent advances in self-powered medical information sensors

Luming Zhao<sup>1,2</sup> | Hu Li<sup>1,3</sup> | Jianping Meng<sup>1</sup> | Zhou Li<sup>1,2,4</sup> 

<sup>1</sup>CAS Center for Excellence in Nanoscience, Beijing Key Laboratory of Micro-nano Energy and Sensor, Beijing Institute of Nanoenergy and Nanosystems, Chinese Academy of Sciences, Beijing, China

<sup>2</sup>School of Nanoscience and Technology, University of Chinese Academy of Sciences, Beijing, China

<sup>3</sup>School of Biological Science and Medical Engineering, Beihang University, Beijing, China

<sup>4</sup>Center on Nanoenergy Research, School of Physical Science and Technology, Guangxi University, Nanning, China

## Correspondence

Zhou Li, Beijing Institute of Nanoenergy and Nanosystems, Chinese Academy of Sciences, Beijing, 100083, China.  
Email: zli@binn.cas.cn;

## Funding information

National Key R&D Project from Minister of Science and Technology, Grant/Award Number: 2016YFA0202703; National Natural Science Foundation of China, Grant/Award Numbers: 21801019, 31571006, 61875015, 81601629

## Abstract

Monitoring various medical information distributed throughout the body is of great importance in early clinic diagnosis and treatment of disease. To discover abnormal medical signals and find their causes in good time, the human body should be monitored continuously and accurately. To meet the requirements, various battery-less and self-powered information acquisition techniques are invented. In this review, the recent advances in self-powered medical information sensors (SMIS) with different functions, structure design, and electric performance are summarized and discussed. The SMIS mainly involves triboelectric nanogenerator (TENG), piezoelectric nanogenerator (PENG), pyroelectric nanogenerator (PyNG)/ thermoelectric generator (TEG) and solar cell. Additionally, this review also analyzed the remaining challenges and prospected the development direction of SMIS in future.

## KEYWORDS

medical information, piezoelectric nanogenerator, self-powered sensor, solar cells, thermoelectric generators, triboelectric nanogenerator

## 1 | INTRODUCTION

In human body, organs and tissues perform different functions to maintain body alive and carry out normal activities. Their physical characteristics can be reflected in various physiological signals that contain abundant medical information for disease diagnosis. Through timely monitoring these physiological signals, medical information closely related to human's healthy state can

be obtained, which is of great importance in preventing diseases in its early stage, recovering of the patients, and maintaining good health.<sup>1-3</sup>

The existing medical information sensing instruments include finger clip oximeter, electrocardiograph (ECG) monitor, sphygmomanometer, electroencephalograph (EEG), infrared radiation thermometer, glucometer in vitro, and gastroscope, enteroscopy, cystoscopy in vivo. These instruments have many advantages in clinic, for example, high accuracy, easy intuition, and outstanding stability. Among them, some clinical test instruments are

Luming Zhao and Hu Li contributed equally to this work.

This is an open access article under the terms of the Creative Commons Attribution License, which permits use, distribution and reproduction in any medium, provided the original work is properly cited.

© 2019 The Authors. *InfoMat* published by John Wiley & Sons Australia, Ltd on behalf of UESTC.

bulky and expensive, which are not portable and may be unable to monitor signals from moving subjects chronically, especially the signals *in vivo*. For the movable clinical test instruments, batteries usually installed to maintain their normal operation, these power sources usually have a large size, heavy weight, and limited lifetime. To increase the battery capacity to meet the power requirement, it is inevitable to further increase its size and weight, which makes the entire sensor lack of portability.<sup>4,5</sup> To solve this dilemma, battery-less and self-powered medical signal monitoring technology emerged in recent years.<sup>6,7</sup>

Self-powered energy harvesters can convert various types of environmental energy into electrical energy and may replace batteries to some extents.<sup>8-14</sup> The newest literature shows the first technology of a capacitive triboelectric electret that is able to compete with piezoelectricity to harvest ultrasound *in vivo* and power medical implants.<sup>8</sup> Compared with batteries, the self-powered energy harvesters have the advantages of low-cost, small size, light weight, unlimited lifetime, and pro-environment, which avoids missing key abnormal medical signals when the battery was drained. The harvested energy can come from human body and the ambient environment, including motion energy from daily actions, physiological activities of people, thermal energy from the temperature difference between human body and indoor/outdoor heat, solar energy from sunlight or indoor light, and so on. These energies can be converted into electrical energy based on different mechanisms such as triboelectric effect,<sup>15-17</sup> piezoelectric effect,<sup>18</sup> Seebeck effect,<sup>14,19,20</sup> and photovoltaic effect.<sup>21-23</sup> More importantly, the self-powered energy harvesters can not only serve as individual medical sensors,<sup>7,24</sup> but also act as power sources for commercial medical sensors.<sup>4,25-27</sup> By wearing the self-powered sensors *in vitro* or implanting them *in vivo*, the researchers can obtain expected medical information and acquire the healthy state of human body.<sup>28</sup>

The purpose of this review is to summarize various types of self-powered medical information sensors (SMIS) during their rapid development in recent years. The detected medical information by SMIS was analyzed in detail, including respiratory rhythm, exhaled breath, pulse, cardiac signals, blood pressure, body temperature, perspiration composition, and some other signals. The SMIS can be triboelectric nanogenerator (TENG), piezoelectric nanogenerator (PENG), pyroelectric nanogenerator (PyNG), thermoelectric generator (TEG), solar cell and their hybrid devices. The working mechanism, energy source, device structure, electric performance and applications of SMIS were presented in sequence. The potential applications, challenges, and perspectives of SMIS are also remarked in our views. The frame of this review is shown in Figure 1.

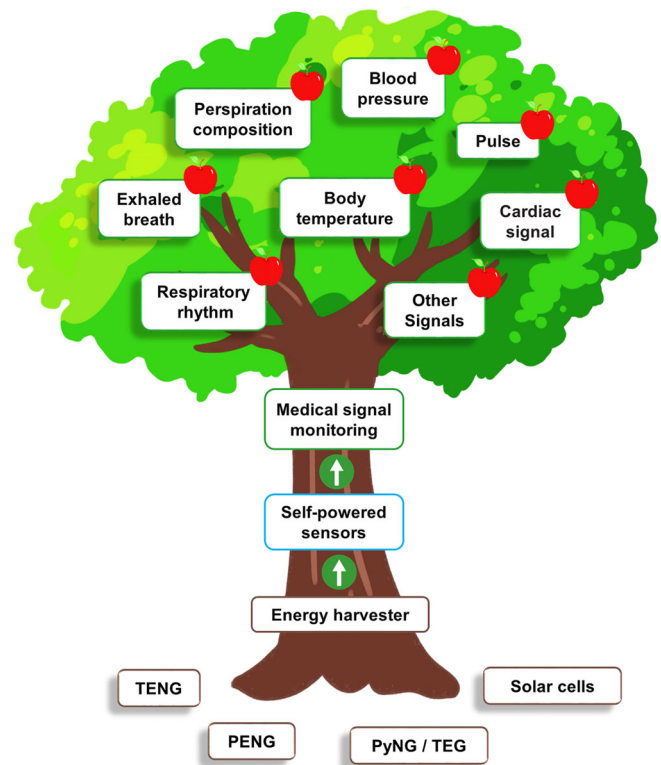


**FIGURE 1** Energy sources of self-powered sensors and the different medical signals detected by the self-powered sensors

## 2 | WORKING MECHANISM OF SELF-POWERED ENERGY HARVESTER

In this review, the self-powered energy-harvesters are divided into four types according to the source of energy. The first two types of the energy-harvesters are TENG and PENG, which are mainly used to harvest motion energy based on triboelectric effect and piezoelectric effect, respectively.<sup>15-18</sup> These motion energy sources varied from essential daily movements to physiological activities, for example, touch,<sup>29</sup> walk,<sup>4</sup> breath,<sup>24</sup> heart beating,<sup>30</sup> internal movement of organs.<sup>31</sup> Except the motions, heat and sunlight are the other two important energy sources in environment. To harvest these two energies, pyroelectric nanogenerator (PyNG)/thermoelectric generator (TEG), and solar cell have emerged in this context. When human body is in a low/high-temperature environment, temperature gradient can be formed between body and indoor/outdoor heat. Once a temperature gradient is formed, the PyNG/TEG can harvest thermal energy based on the Seebeck effect.<sup>14,19,20</sup> For the energy from sunlight or indoor light, it can be converted into electricity by solar cells based on photovoltaic effect.<sup>21-23</sup> The working mechanisms of TENG, PENG, PyNG/TEG, and solar cell will be described in detail in following sections.

## 2.1 | Triboelectric nanogenerator

The energy harvesting ability of TENG comes from the conjunction of triboelectrification and electrostatic induction between two friction layers.<sup>32-34</sup> The constituent materials of the friction layers have different electron-attracting abilities. When they are brought into contact, opposite signs of triboelectric charges are generated at these two friction surfaces. After the friction layers are separated by an external force, a potential drop can be induced by the opposite signs of triboelectric charges, it varies as the triboelectric surfaces contact and separate from each other. To balance the potential difference, the free electrons flow back and forth through the connected external circuit. Generally, the TENGs have four different fundamental working modes on the basis of device structure and working manner (Figure 2), including vertical contact-separation mode, lateral sliding mode, single-electrode mode, and freestanding triboelectric-layer mode.

### 2.1.1 | Vertical contact-separation mode

In 2012, the TENG was first invented with the vertical contact-separation mode (Figure 2A).<sup>15</sup> Two films with different electron-attracting abilities serve as friction layers, and metallic electrodes are deposited on the back surfaces of the friction layers. After an external force makes two friction surfaces of TENGs contact and rub, oppositely

charged surfaces are created. Once the force is withdrawn, the two friction layers are subsequently separated, an electric potential difference is generated at the interface region, which can drive free electrons flow from an electrode to another. As the gap of friction layers vanishes, the potential difference also disappears due to the backflow of free electrons. Therefore, during the periodically pressing and releasing of the TENG, free electrons flow back and forth, which generates alternative current pulse output.<sup>35,36</sup>

### 2.1.2 | Lateral-sliding mode

Figure 2B shows the initial structure of lateral-sliding mode, similar to that of vertical contact-separation mode. When the two friction surfaces contact and align with each other, no electric potential difference exists at the interface region because triboelectric charges are completely compensated. When a relative displacement takes place along parallel direction, triboelectric charges cannot be completely compensated, giving rise to an electric potential difference across the two electrodes.<sup>37,38</sup> With periodical sliding apart and closing, the TENG with lateral-sliding mode can produce alternative current pulse output. The lateral-sliding mode has the advantage of more effective triboelectric charges transfer compared with the first working mode. Additionally, besides the planar motion in Figure 2B, the lateral-sliding mode can also be disc rotation<sup>39</sup> and cylindrical rotation.

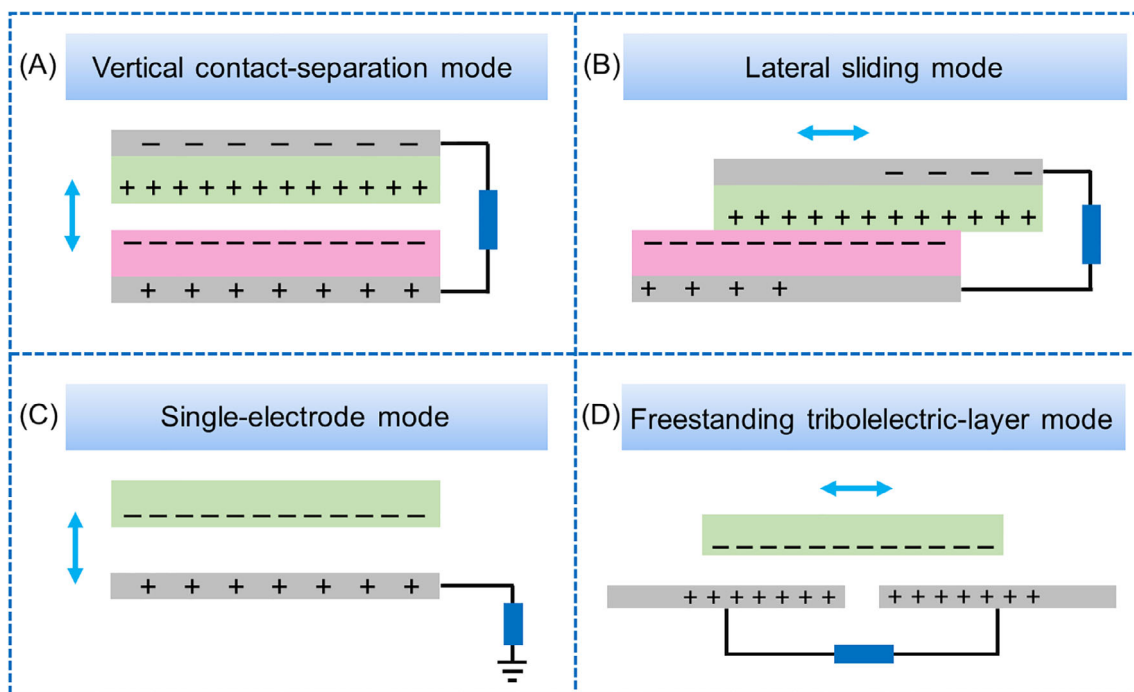


**FIGURE 2** Four fundamental working modes of TENG. A, Vertical contact-separation mode. B, Lateral-sliding mode. C, Single-electrode mode. D, Freestanding triboelectric-layer mode

### 2.1.3 | Single-electrode mode

The two aforementioned working modes have two friction layers and two electrodes interconnected by an external circuit, which limit their versatility and applicability when harvesting energy from a freely moving object. Figure 2C shows a single-electrode mode that can be used for this application scenario. The single-electrode mode consists of a moving object and a bottom electrode electrically connected to the ground. When the top object approaches and departs from the bottom electrode, the local electrical field distribution will be changed. To match the potential change, electrons are driven to flow between the ground and the bottom electrode, which generates alternating current along the external circuit. This energy harvesting strategy can also be applied in both vertical contact-separation mode and lateral-sliding mode.<sup>40,41</sup>

### 2.1.4 | Freestanding triboelectric-layer mode

The TENG with freestanding triboelectric-layer mode can also be used to harvest mechanical motion energy without an attached electrode. As shown in Figure 2D, the freestanding triboelectric-layer mode consisted of a pair of symmetric electrodes under a dielectric film, and the sizes of the electrodes are of the same order as the size of the moving object. Additionally, there is a small gap between the dielectric film and the electrode. The dielectric film is precharged by friction, when the dielectric film gets close to the electrodes, equal amounts of opposite charges distribute on the lower electrodes. The forward and backward movements of dielectric film break the balance of charge distribution of two electrodes, then a potential difference formed, which impels the free electrons flow back and forth in the external circuit. This process leads to the generation of alternating current along the external circuit.<sup>42,43</sup>

## 2.2 | Piezoelectric nanogenerator

Different from TENG, PENG is another widely used energy-harvesting technology based on the piezoelectric effect (Figure 3). When applying an external force to piezoelectric materials, internal piezoelectric potential can be formed due to the generation of electric dipole moments. Taking the common zinc oxide (ZnO) crystal as an example, its atomic model is shown in Figure 3A, the tetrahedrally coordinated  $\text{Zn}^{2+}$  and  $\text{O}^{2-}$  are accumulated layer-by-layer along the  $c$ -axis. In the initial state, the  $\text{Zn}^{2+}$  cations are overlapped with the center of the  $\text{O}^{2-}$  anions.

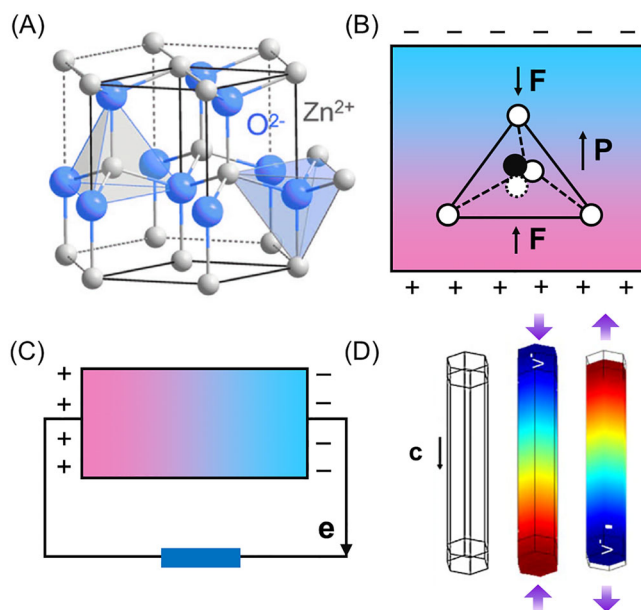


**FIGURE 3** Structure and working principle of a ZnO-based PENG. A, Atomic model of the wurtzite-structured ZnO.<sup>11</sup> B, Dislocation of a compressive ZnO nanowire. C, Diagram of piezoelectric principle. D, Piezoelectric potential calculation of axial-strained a ZnO nanowire. Reproduced with permission.<sup>44</sup> Copyright 2018, AIP Publishing Group

Once a strain along the  $c$ -axis is applied, the centers of the  $\text{Zn}^{2+}$  cations and  $\text{O}^{2-}$  anions are dislocated, inducing an electric dipole and resulting in a piezoelectric potential in ZnO, which drives the free electrons flow through the external circuit (Figure 3B,C).<sup>45</sup> When applying compressive or tensile strain to a ZnO nanowire along the  $c$ -axis, positive and negative piezoelectric potentials are generated at the two ends of the nanowire, respectively (Figure 3D). Through applying a dynamic external force periodically, piezoelectric potential can be altered sequentially, which contributes to the alternative pulse current flowing through the external circuit continuously.<sup>46</sup> Piezoelectric materials and flexible substrates are two key elements for constituting PENG, through selecting piezoelectric materials and optimizing device structure, the sensing performance of PENG-based medical sensors can be further improved.

## 2.3 | PyNGs/TEG

Besides the motion energy, thermal energy is also a kind of widespread energy source, but it is often neglected and wasted in our daily life. To fully gather the waste thermal energy, PyNG/TEG is invented to convert thermal energy into electricity based on the spin Seebeck effect (Figure 4A). As shown in the upper inset in Figure 4A, the thermocouple is composed of two metals A and B with different Seebeck coefficients, the temperature

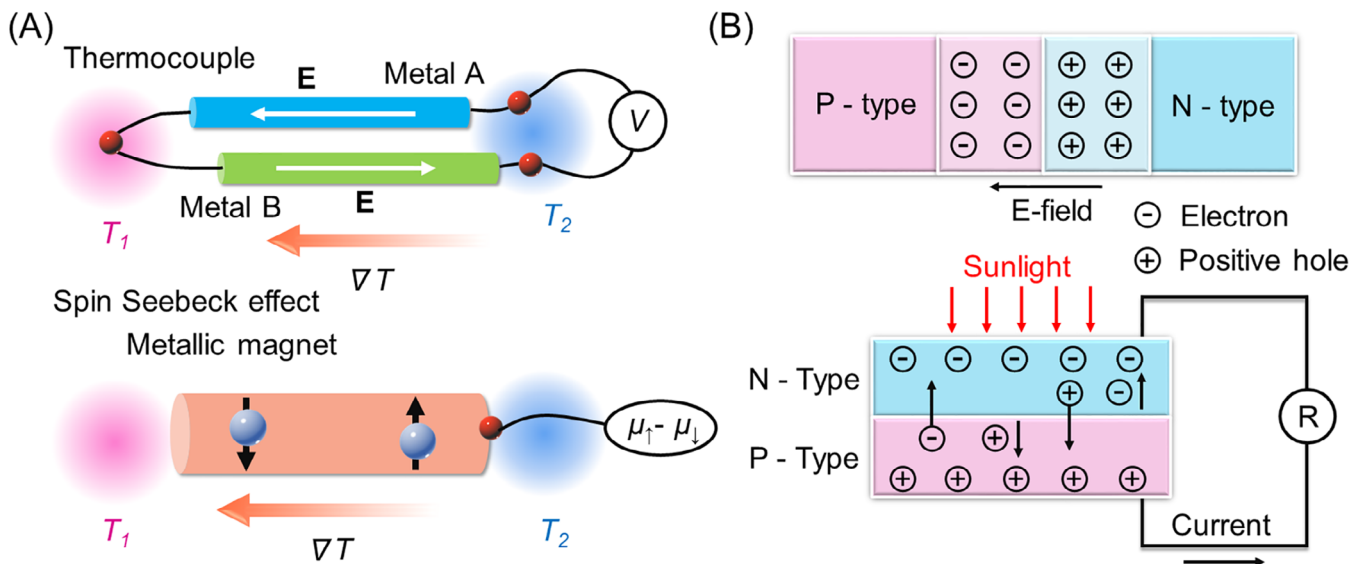


**FIGURE 4** A, Working mechanism of PyNG/TEG based on spin Seebeck effect. B, Working mechanism of the photovoltaic solar cell

difference  $\Delta T$  ( $T_1 - T_2$ ) can result in an electric voltage ( $V$ ) between the output terminals. Additionally, through placing a metallic magnet under a temperature gradient, the internal carriers move from the hot end ( $T_1$ ) to the cold end ( $T_2$ ), and then accumulate at the cold end, resulting in a spin voltage ( $\mu_{\uparrow} - \mu_{\downarrow}$ ) along the temperature gradient (lower inset in Figure 4A).<sup>19</sup>

Compared with the TENG and PENG, PyNG/TEG-based sensors are more sensitive to the signals related with temperature change. In many application scenarios, PyNG/TEG itself can be used as a medical information sensor. It can also be used to harvest energy derived from the temperature difference between body and ambient, and then work as a power source to provide electricity for other medical information sensors.

## 2.4 | Photovoltaic solar cell

Solar energy is a common energy source from nature; it can be directly collected and converted by solar cells. The energy harvesting ability of solar cell comes from the photovoltaic effect of PN junction (Figure 4B). At the interface of PN junction, the N-type semiconductor has plenty of free electrons, which will diffuse to P-type semiconductor. The P-type semiconductor has plenty of holes, which will diffuse to N-type semiconductor. This process make the N-type semiconductor positively charged, and the P-type semiconductor negatively charged at the interface. A built-in electric field pointed from N-type semiconductor to P-type semiconductor can be formed at the PN junction interface (upper inset in Figure 4B). When the sun shines on the PN junction, electron-hole pairs are formed at the interface of PN junction, under the action

of built-in electric field, electrons migrate to N-type semiconductor, the holes migrate to P-type semiconductor. Therefore, N-type and P-type semiconductors accumulate excessive electrons and holes, respectively, which offset the built-in electric field and make the N-type and P-type be negatively charged and positively charged, respectively. Potential difference can be formed at the PN junction and make the free electrons generate periodic flow through the external circuit.<sup>21-23</sup> In practical applications, for serving as the power unit of the self-powered medical signal sensor, the solar cells should be further optimized to be more effective and miniaturized.

## 3 | SELF-POWERED SENSORS FOR MEDICAL SIGNALS DETECTION

In this review, the self-powered functions of SMIS are achieved by two approaches. In the first case, the energy harvesters themselves serve as independent sensors and achieve the sensing function, they directly convert the detected physiology activities into electric medical signals. For instance, TENG- or PENG-based sensors can be worn on or implanted in body to detect physiology signals related to motion energy varying from breath, pulse to the internal activities of organs. PyNG/TEG-based sensors can be worn on body to detect medical signals related to body temperature. In the second case, the energy harvesters can be used as a power source to provide energy for other sensors, for example, the motion energy, thermal energy and even solar energy deriving from human activities and surrounding environments can also be harvested and stored to power commercial sensors and monitor medical signals without batteries. In

this section, the typical SMIS are summarized and introduced in detail based on the types of detected physiology signals, including the detection object, device structure, materials selection, and electric performance.

### 3.1 | Self-powered breath sensors

As one of the most important behaviors from human body, respiration plays a key role in keeping normal physiological activities, its monitoring and analyses are of great value for physical health management and clinical diagnosis.<sup>24,51-59</sup> To achieve the real-time monitoring and analyses, various self-powered respiratory sensors are designed to be portable and miniaturized.<sup>52-54</sup> By the monitoring of respiratory rhythm and exhaled breath, the cardiac or arterial vascular function and internal diseases can be effectively diagnosed. This process has great clinic significance on early diagnosis and treatment of many diseases.

#### 3.1.1 | Self-powered respiratory rhythm sensors

In 2018, Wang et al designed an air-flow-driven TENG that can realize self-powered respiratory rhythm monitoring through converting breathing energy into electrical signals (Figure 5A).<sup>24</sup> The TENG consisted of a flexible polytetrafluoroethylene (n-PTFE) film and two copper (Cu) film electrodes, one end of the n-PTFE film was fixed at the middle of an acrylic tube. A Cu film was attached on

the bottom surface of the acrylic tube. Another thin Cu film was attached on the top of the n-PTFE film serving as the back electrode. The n-PTFE film can be oscillated and continuously contact/separate with the Cu film on the bottom of the acrylic tube during the process of air flow. The output performance of the TENG increased with air flow rates. Therefore, the TENG can be installed in a conventional medical mask to monitor human breath in real time. The parameters of its output electrical signals were different under different breathing patterns. For instance, when the self-powered respiratory sensor was exposed to slow, rapid, shallow, and deep breathing patterns, the voltage peaks are 1.2 V, 1.8 V, 0.2 V, and 1.3 V, respectively. Additionally, the TENG-based respiratory sensor can be integrated with a wireless signal processing and transmission system, which realized remote and real-time respiratory monitoring. The converted electric energy by TENG can also be stored in a supercapacitor and used to measure the responsivity of the strain sensor to respiratory behaviors.

Besides TENG, PENG can also be used to detect human breath. In 2018, Wang et al fabricated a flexible piezoelectric pressure sensor using a poly(vinylidene fluoride-trifluoroethylene) and multiwalled carbon nanotube (P[VDF-TrFE]/MWCNT) composite film (Figure 5B).<sup>47</sup> The PENG-based pressure sensor was sensitive to the external force. When it was clamped under the nose, due to the action of the respiratory airflow, the sensor can be deformed and generate voltage pulses whose value and frequency were approximate 0.1 V and 0.68 Hz, respectively. The value and frequency of the voltage peaks changed in response to the depth and rhythm of respiration, respectively.

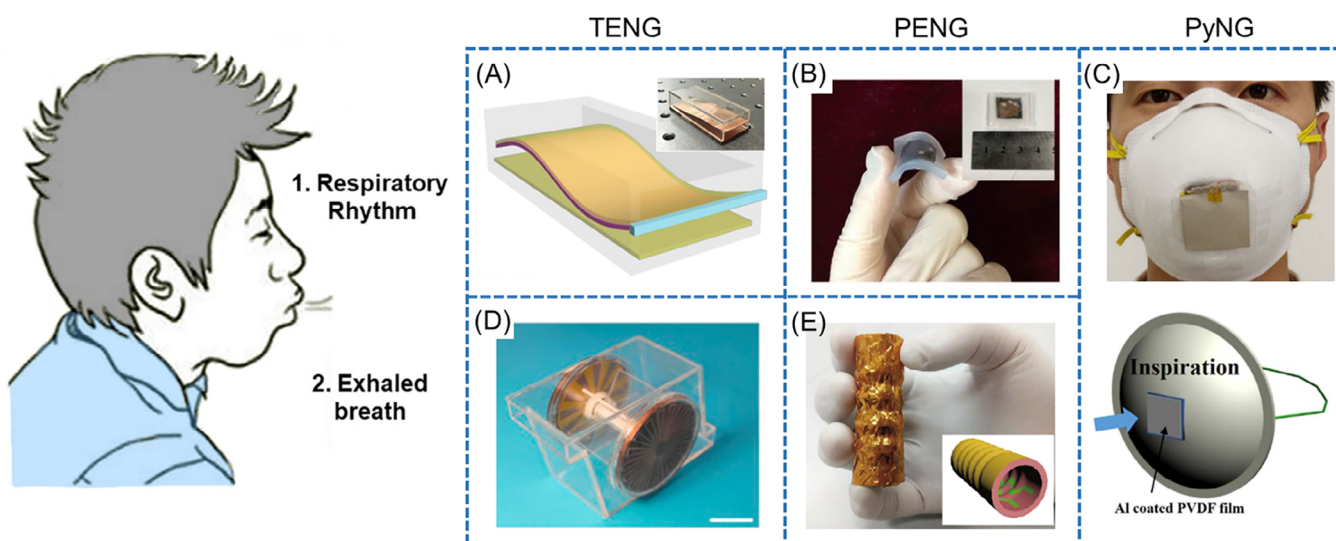


**FIGURE 5** Self-powered real-time respiratory rhythm sensors based on (A) air-flow-driven TENG,<sup>24</sup> (B) PENG<sup>47</sup> and (C) PyNG.<sup>48</sup> Reproduced with permission.<sup>24</sup> Copyright 2018, American Chemical Society. Reproduced with permission.<sup>47</sup> Copyright 2018, MDPI Publishing Group. Reproduced with permission.<sup>48</sup> Self-powered breath analyzers based on (D) blow-driven TENG<sup>49</sup> and (E) PENG arrays.<sup>50</sup> Reproduced with permission.<sup>49</sup> Copyright 2015, Elsevier Publishing Group. Reproduced with permission.<sup>50</sup> Copyright 2018, Springer Nature Publishing Group

Unlike TENG- and PENG-based breath sensors, which achieve self-powered respiratory rhythm monitoring through converting respiratory airflow into electric signals, the detection function of PyNG-based breath sensors were realized by converting the temperature fluctuation into electrical signals. In 2017, Xue et al fabricated a wearable self-powered PyNG-based sensor (Figure 5C).<sup>48</sup> A PVDF film with the size of 3.5 cm × 3.5 cm was chosen as the core pyroelectric component of the PyNG, two aluminum (Al) films attached on both surfaces of the PVDF film acted as electrodes. Due to the pyroelectric effect, the output performance of the PyNG was closely related with the temperature difference formed between the exhaled gas and ambient temperature. When mounting the PyNG on a respirator, it can directly record the respiratory rate and generate electrical output of 2.5  $\mu$ A and 42 V at ambient temperature of 5°C. Three different kinds of breathing patterns, including deep breathing, normal breathing, and rapid breathing, can be distinguished by the PyNG-based breath sensor. Additionally, it can also be used to detect the ambient temperature and harvest wearable energy to power other electric devices.

### 3.1.2 | Self-powered breath analyzers

In aforementioned cases, TENG and PENG themselves directly acted as self-powered respiratory rhythm sensors by converting the respiratory movement into electric signals. In addition to the self-powered sensing function, the TENG and PENG can also be used as the power source for breathed-out gas sensor and achieve the self-powered breath analyzing.<sup>49,50,56</sup>

In 2015, Wen et al fabricated a blow-driven triboelectric nanogenerator (BD-TENG) as the power source for active exhaled alcohol gas detection (Figure 5D).<sup>49</sup> The cobalt oxide ( $\text{Co}_3\text{O}_4$ ) was used to detect the gas concentration for its sensitive resistance variation with the ambient alcohol concentration. The BD-TENG had a disc rotation sliding mode and can induce electricity when it was driven by the blowing air. The output voltage of BD-TENG was free from blowing speed, which may eliminate the interference of breathing patterns and be suitable for gas sensing. The resistance of the  $\text{Co}_3\text{O}_4$ -based gas sensor increased with the ambient alcohol concentration, the voltages applied over the gas sensor by the BD-TENG also increased with increasing the alcohol concentrations. The BD-TENG based gas sensing system can detect alcohol with a low concentration of 10 ppm, and its response to 100 ppm alcohol vapor is  $\sim 34.5$  at the optimized working temperature (ie, 160°C). Additionally, the BD-TENG based gas sensor showed great selectivity for alcohol detection through testing with other similar gases. When the BD-

TENG was blown by a drinking person gently, an alarm system can be triggered by the generated voltage and emit a warning signal. Recently, Zhong et al fabricated a body-motion-driven TENG-based smell detector,<sup>60</sup> this smell detector can generate triboelectric current outputs like specific code and thus differentiate various gas species (methanol, ethanol, acetone, toluene, and chloroform vapor). A series of triboelectric-sensing signal can act as different neural stimulation to mouse brain, mouse body can respond to the stimuli and make corresponding particular behaviors. This new research effectively promoted the development of closed-loop human-machine interactions.

In 2018, Fu et al developed a self-powered breath analyzer using polyaniline/polyvinylidene fluoride (PANI/PVDF) arrays for exhaled breath analysis (Figure 5E).<sup>50</sup> The sensor achieved its self-powered gas-sensing function by converting exhaled breath into piezoelectric signals. The PVDF film served as a PENG and powered the gas-sensing system due to its piezoelectric effect. Five individual PANI patterns with different dopant sources served as both electrodes and different gas-sensing elements. The PANI/PVDF piezoelectric bellows can be used to detect the different gases (eg, alcohol, acetone, CO,  $\text{CH}_4$ , and  $\text{NO}_x$ ) with concentration from 0 to 600 ppm at room temperature, it also showed potential in detecting gas markers from exhaled breath for disease diagnosis.

Table 1 summarized various SMIS for respiration monitoring, including the sensor types, function in sensing system, output performance, device size, monitoring position, and constituent materials. According to these studies, the TENG, PENG, PyNG, and their hybrid device have been used for respiration monitoring, the solar cell has not been report yet in this application scenario. The TENG can not only be used as individual sensors but also energy supplier that can harvest breathing energy into electrical energy. The other types of devices were usually used as individual sensors. The output values of TENG (eg, several volts) are generally higher than that of PENG (eg, several millivolts) due to the stronger triboelectric effect of TENG. The collected signal can be voltage, current, or charge quantity. The sizes of these devices focused on an order of centimeter. The monitoring positions varied from in vitro to in vivo. The monitoring positions of TENG and PENG are active and movable, which can generate physiological activities. The monitoring positions of PyNG relied on an assistive device that can fix it near mouth. Compared with PyNG, the constituent materials of TENG and PENG are more extensive and available. Additionally, the application scenes of PyNG are limited by the environmental temperature. In future, a miniaturized dimension and high output will be the research target for self-powered breath sensors. Additionally, the self-powered breath sensors sensitive to multiple gases or even mixed gases can be further developed.

**TABLE 1** Summary of self-powered sensors for respiration monitoring

| Type                 | Single energy harvester   |  |  | Hybrid                               |  |  |
|----------------------|---|--|--|--------------------------------------|--|--|
|                      | TENG  |  | PENG   | PyNG                                 | PE/TENG  | Py/PE/TENG   |
| Function             | Sensor  | Power source   | Sensor   | Sensor                               | Sensor   | Sensor   |
| Output               | 2 V, <sup>24</sup> 0.2 V, <sup>52</sup> 0.6 V, <sup>53</sup><br>4 V, <sup>54</sup> 5 V, <sup>55</sup>   | 0.1 V, <sup>49</sup><br>$\Delta R/R_0 = 2\%$ <sup>61</sup>                                       | 0.1 V, <sup>47</sup> 10 nA, <sup>50</sup><br>100 mV, <sup>62</sup> 2 mV, <sup>63</sup>   | 42 V <sup>48</sup>                   | 0.1 V <sup>64</sup>  | 25 V <sup>65</sup>   |
| Size/cm <sup>2</sup> | 5.5 × 2, <sup>24</sup> 4.5 × 4.5, <sup>52</sup><br>1 × 2, <sup>53</sup> 3.3 × 3.3, <sup>54</sup><br>1.2 × 1.2 <sup>55</sup>   | Φ 5 cm, <sup>49</sup><br>4 × 2 <sup>61</sup>   | 1.5 × 1.5, <sup>47</sup> 5 × 5, <sup>50</sup><br>3 × 2.5 <sup>62</sup>   | 3.5 × 3.5 <sup>48</sup>              | 2.5 × 3 <sup>64</sup>  | 3.5 × 3 <sup>65</sup>  |
| Position             | Mouth, <sup>24</sup> mask, <sup>24,53</sup><br>back, <sup>52</sup> chest, <sup>54</sup> left<br>chest, rat <sup>55</sup>  | Mouth, <sup>49</sup> neck <sup>61</sup>  | Under nose, <sup>47</sup><br>mouth, <sup>50</sup> throat, <sup>62</sup><br>diaphragm, rat. <sup>63</sup>   | Mask <sup>48</sup>                   | Belly <sup>64</sup>  | Throat, <sup>65</sup><br>mask <sup>65</sup>                    |
| Materials            | PTFE, <sup>24</sup> Cu, <sup>24,54</sup><br>Acrylic, <sup>24</sup> FEP, <sup>52,54</sup><br>SPS, <sup>52</sup> EVA, <sup>52</sup> Ag, <sup>52,53</sup><br>PVDF, <sup>53</sup> PDMS <sup>54,55</sup><br>Au, <sup>55</sup> Al <sup>55</sup> | Au, <sup>49</sup> FEP, <sup>49</sup><br>PEDOT:PSS/PU, <sup>61</sup><br>AgNWs, PDMS <sup>61</sup> | P(VDF-TrFE)<br>/MWCNT, <sup>47</sup><br>PANI, <sup>50</sup> PVDF, <sup>50</sup><br>BCST, <sup>62</sup> PDMS, <sup>62</sup><br>ZnO NW <sup>63</sup> | PVDF, <sup>48</sup> Al <sup>48</sup> | P(VDF-TrFE), <sup>64</sup><br>PDMS, <sup>64</sup> PU, <sup>64</sup><br>CNTs & Ag <sup>64</sup> | PDMS, <sup>65</sup><br>PVDF, <sup>65</sup><br>Ag <sup>65</sup> |

Note: PE/TENG represents hybrid PENG and TENG. Py/PE/TENG represents hybrid PyNG, PENG, and TENG.

### 3.2 | Self-powered cardiovascular system sensors

Following the accelerated speed of population aging, cardiovascular diseases, including heart diseases and vascular diseases, have become one of the greatest threats to human health.<sup>66,67</sup> Fortunately, most of them can be diagnosed in advance by various medical sensors. Timely monitoring of physiological signals in vitro and in vivo, such as heart rate,<sup>25,52,57,63,65,68-71</sup> electrocardiograph (ECG),<sup>4,26,27</sup> radial artery pulse<sup>52,54,58,69,72-77</sup> and blood pressure,<sup>69,71,78,79</sup> can provide effective information of personal health status, some of the cardiovascular diseases can be prevented by early treatment. In clinical practice, the sudden changes in vital signs are life-threatening. To avoid missing these key medical information, the physiological signals should be recorded in real-time continuously. In order to achieve this goal, plenty of wearable, miniaturized, implantable self-powered cardiovascular sensors with high sensitivity have been developed.

#### 3.2.1 | Wearable self-powered pulse, heart rate, and ECG sensors

Radial artery pulse, heart rate and ECG carry many medical information of cardiovascular status. These medical signals can be monitored in vitro by wearable self-powered sensors. Among them, the radial artery pulse can be detected on the wrist. Its amplitude, frequency, and waveform are significant parameters of the cardiovascular.

In 2017, Ouyang et al proposed a TENG-based flexible self-powered ultrasensitive pulse sensor (SUPS) that can directly convert the human pulse vibration signals into electrical signals (Figure 6A).<sup>72</sup> The SUPS consisted of two nanostructured Kapton films, one Kapton film had an ultrathin Cu layer on the its back side, the other Kapton film was totally covered by an ultrathin Cu film. The SUPS has a size of 2 cm × 1 cm, it was encapsulated by polydimethylsiloxane (PDMS) to enhance its stability. The SUPS showed excellent sensing performance when it was pressed on the radial artery, its output voltage was 1.52 V, the response time was as fast as 50 μs, and the signal-noise ratio was 45 dB. Through analyzing the obtained pulse waveforms, the SUPS was demonstrated to show high accuracy in heart rate monitoring and can be used to indicatively diagnose cardiovascular diseases such as arrhythmia, coronary heart disease, and atrial septal defect. Additionally, the SUPS can be integrated with a bluetooth chip to achieve mobile, wireless, and real-time monitoring of radial artery pulse signals.

In 2017, Park et al demonstrated a PENG-based flexible self-powered pulse sensor with high sensitivity. Its core component was a thin Pb[Zr<sub>x</sub>Ti<sub>1-x</sub>]O<sub>3</sub> (PZT) film with gold interdigitated electrodes (Figure 6B).<sup>80</sup> The output voltage of the as-fabricated PZT-based sensor varied linearly with the applied pressure (pressure sensitivity: 0.018 kPa<sup>-1</sup>) under the pressure of 30 kPa. The response time of the piezoelectric pressure sensor was 60 ms, which ensured the pressure sensor response to rapid variation of dynamic pressure timely. When attached the piezoelectric pressure sensor on a human wrist and neck, it

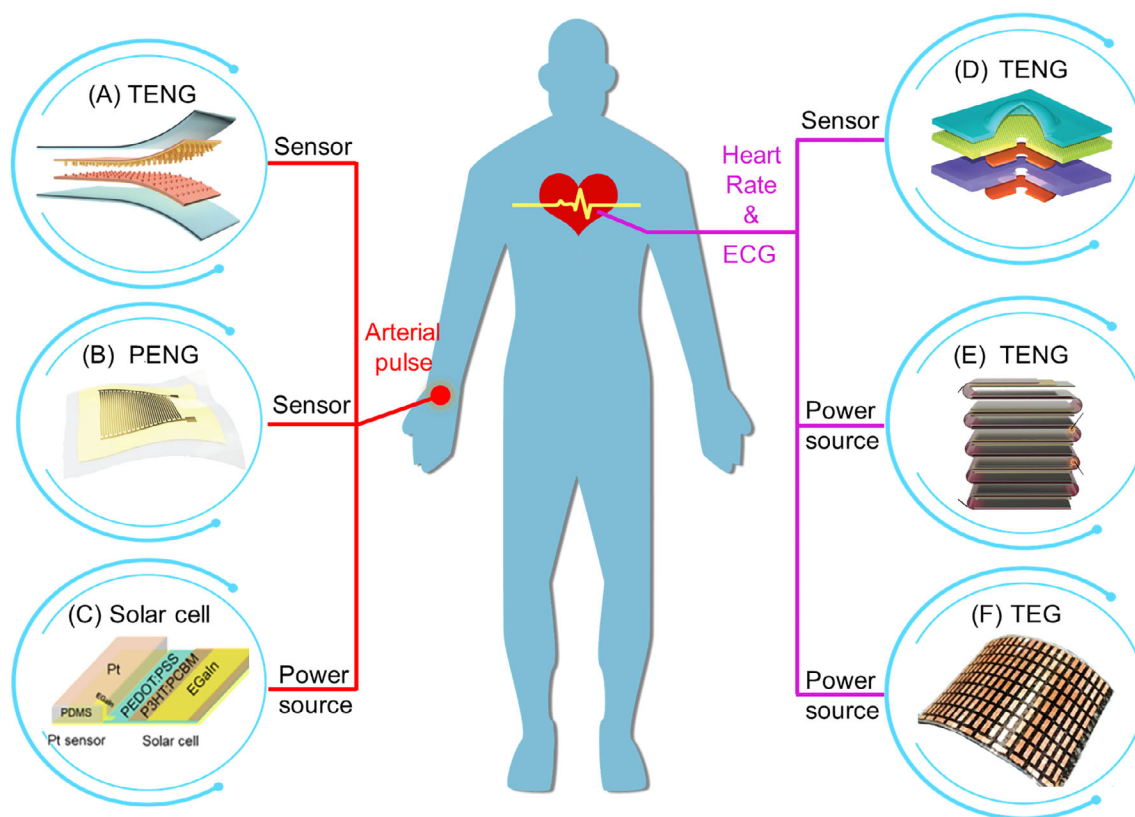


**FIGURE 6** Self-powered real-time radial artery pulse sensors based on (A) TENG<sup>72</sup> and (B) PENG.<sup>80</sup> Reproduced with permission.<sup>72</sup> Copyright 2017, John Wiley & Sons. Reproduced with permission.<sup>80</sup> Copyright 2017, John Wiley & Sons. C, Solar cell as a power source for self-powered real-time radial artery pulse sensors. Reproduced with permission.<sup>81</sup> Copyright 2018, American Chemical Society. D, TENG as self-powered real-time heart rate and ECG sensors. Reproduced with permission.<sup>57</sup> Copyright 2014, John Wiley & Sons. E, TENG<sup>4</sup> and F, PyNG<sup>26</sup> as power sources for self-powered real-time heart rate and ECG sensors. Reproduced with permission.<sup>4</sup> Copyright 2015, Springer Nature Group. Reproduced with permission.<sup>26</sup> Copyright 2018, American Chemical Society

can be deformed and generate voltage signals responded to radial/carotid artery movements and respiratory activities. The peak-to-peak voltage and frequency of the artery pulse signal before exercise were 65 mV and about 73 beats per minute. Various important physiological information, such as heart rate, arterial stiffness, coronary artery disease and myocardial infraction, can be extracted from the obtained artery pulse signals. Similar with the SUPS, the PENG-based pulse sensor can also monitor radial artery pulse signals wirelessly in real-time through being integrated with a bluetooth chip.

Different from TENG and PENG, the energy sources of PyNG/TEG and solar cell are thermal energy and light that can be converted into electrical energy and stored to power the sensors continuously. In 2018, Hsieh et al reported a flexible and wearable tactile sensing device, which was composed of a Pt strain sensor in series with an organic solar cell (Figure 6C).<sup>81</sup> The resistance of the Pt crack-based strain sensor increased when bent outward and decreased when bent inward. The solar cell can provide enough power to drive the Pt strain sensor under

indoor light illumination ( $2 \text{ mW cm}^{-2}$ ), which enabled this coplanar device to realize self-powered real-time human physiological signals monitoring. When attaching the sensing device on the wrist, cardiovascular information including the systolic and diastolic movements of the heart can be obtained in the form of acceptable and readable output electric signals.

Heart rate is a direct reflection of the health status of the human cardiovascular system, various methods have been developed to monitor it. Besides above human wrist, the monitoring position can also be the chest. In 2014, Bai et al fabricated a membrane-based self-powered TENG-based sensor (M-TES) that can be used for heartbeat monitoring (Figure 6D).<sup>57</sup> The M-TES consisted of a piece of acrylic substrate, two circular Cu electrodes, a fluorinated ethylene propylene (FEP) film with arranged nanorod arrays on its surface, and a latex membrane intimately contact with the FEP film. The M-TES was demonstrated to be sensitive to dynamic air pressure change. When air pressure was in the range of 2.9 to 3.4 KPa, the electric potential

difference of the M-TES with apparent areas of  $3.2 \text{ cm}^2$  was linear with the air pressure, and the average sensitivity was  $0.33 \text{ V KPa}^{-1}$ . Heartbeat induced periodical air pressure change in a chest piece can be detected by the M-TES due to its high resolution. Each heartbeat can be monitored by a voltage pulse signal of about  $0.06 \text{ V}$ , the measured heartbeat rate of the subject was 72 times per minute which is the same with the counting results. Additionally, a normal breathing rate of 32 times per minute can also be detected by the M-TES.

Sometimes, when the heart beating is weak, it is hard to achieve direct monitoring on skin just by a TENG. For these application scenarios, the researchers can detect the signals in virtue of a commercial heart-rate sensor. The TENG can be used as a power source by harvesting motion energy on other positions and provide electricity for the sensor.

In 2015, Niu et al reported a high-efficient self-charging power system based on a high-output TENG (Figure 6E).<sup>4</sup> The TENG with multilayer structure was composed by AI and FEP films, which had the advantage of small volume and lightness. When embedded in the shoe insoles, the multilayered TENG can scavenge energy from human walking and running and generate a voltage of  $700 \text{ V}$ . Through integrating with a power management circuit, the theoretical total efficiency  $\eta_{\text{total}}$  can be calculated using the formula:  $\eta_{\text{total}} = P_{\text{store,avg}}/P_{\text{R,avg,opt}}$ , where  $P_{\text{store,avg}}$  represents the maximum d.c. power stored into the storage unit;  $P_{\text{R,avg,opt}}$  represents the maximum a.c. power delivered to a resistive load. The  $P_{\text{store,avg}}$  and  $P_{\text{R,avg,opt}}$  measured in experiment were  $0.2023 \text{ mW}$  and  $0.3384 \text{ mW}$ , respectively, and the calculated  $\eta_{\text{total}}$  was 60%. A continuous direct current electricity of  $1.044 \text{ mW}$  can be obtained by the TENG-based power unit, an ECG system was successfully powered that realized self-powered ECG signal monitoring.

In 2018, Kim et al developed a wearable self-powered ECG monitoring system. In this system, a wearable TEG (w-TEG) was used for real-time electricity generation for wearable ECG module wrapped on human wrist. A flexible heat sink was the essential part to create a temperature difference for the w-TEG (Figure 6F).<sup>26</sup> At the first 10 minutes, the output power density of w-TEG was about  $38 \mu\text{W cm}^{-2}$ . After driving the circuit for 22 hours, the power density was still over  $13 \mu\text{W cm}^{-2}$ . In order to make the ECG module operate regularly, the output voltage of the w-TEG should be boosted by a voltage boost converter, which consumed about 93% of the power supplied by the w-TEG, 7% of the power was left to drive the ECG system. The output power of the w-TEG after 24 hours was about  $1 \text{ mW}$ , 7% of the power (ie,  $70 \mu\text{W}$ ) was high enough to drive the ECG system continuously because its required power is less than  $15 \mu\text{W}$ .

### 3.2.2 | Implantable self-powered cardiovascular and blood pressure sensor

As an invasive method, the wearable sensors can acquire the cardiovascular signals in vitro. However, the signals transmitted through human skin are usually weak and susceptible to body movements. In order to eliminate the interference of human activities and monitor these signals with higher fidelity and accuracy, implantable sensors have been invented to meet this demand.<sup>82-84</sup> Compared with wearable sensors, the obtained signals by implantable sensors convey more detailed medical information. To overcome the drawback low-capacity of battery and achieve long-term cardiovascular signals monitoring in vivo, the self-powered feature for implantable sensors is expected without battery, which avoid the limitation of the battery life and reduce the surgical risk of patients.

To achieve self-powered cardiovascular signals monitoring in vivo, various kinds of biomechanical energy were harvested by implantable devices as either sensors or power sources. In 2016, Ma et al proposed a flexible, implantable, and self-powered TENG-based active sensor (iTEAS) for continuous cardiovascular signals monitoring, the iTEAS can directly convert the biomechanical signals of internal organs into electrical signals (Figure 7A).<sup>71</sup> The as-fabricated iTEAS consisted of two tribo-layers (ie, an AI film and a nanostructured PTFE thin film), an Au electrode layer served as the back electrode of PTFE film and spacers. The iTEAS was encapsulated to make it hermetic and flexible. After implanting and fixing the iTEAS into the pericardial sac of an adult Yorkshire pig, the triboelectric layers contacted and separated with each other due to heart contraction and relaxation. The iTEAS can output electrical signals of  $10 \text{ V}$  and  $4 \mu\text{A}$  during this process. The heart rate detection accuracy of the iTEAS reached to about 99%. The cardiac behaviors can be described accurately by the output waveform of the iTEAS, and life-threatening arrhythmia such as atrial fibrillation and ventricular premature contraction can be detected in time. Additionally, the pressure, velocity of blood flow and respiratory rates could be monitored by the iTEAS in vivo. In 2016, Zheng et al demonstrated an implantable TENG (iTENG) with similar structure and function.<sup>70</sup> The heartbeat-related electrical signals was detected by iTENG. The integrated iTENG-based unit can power a wireless transmission system to achieve self-powered, real-time, and wireless cardiac monitoring.

In addition to the triboelectric devices, the motion energy in vivo can also be harvested by piezoelectric device. The physiological signals can be converted into electrical signals for cardiovascular signals monitoring.

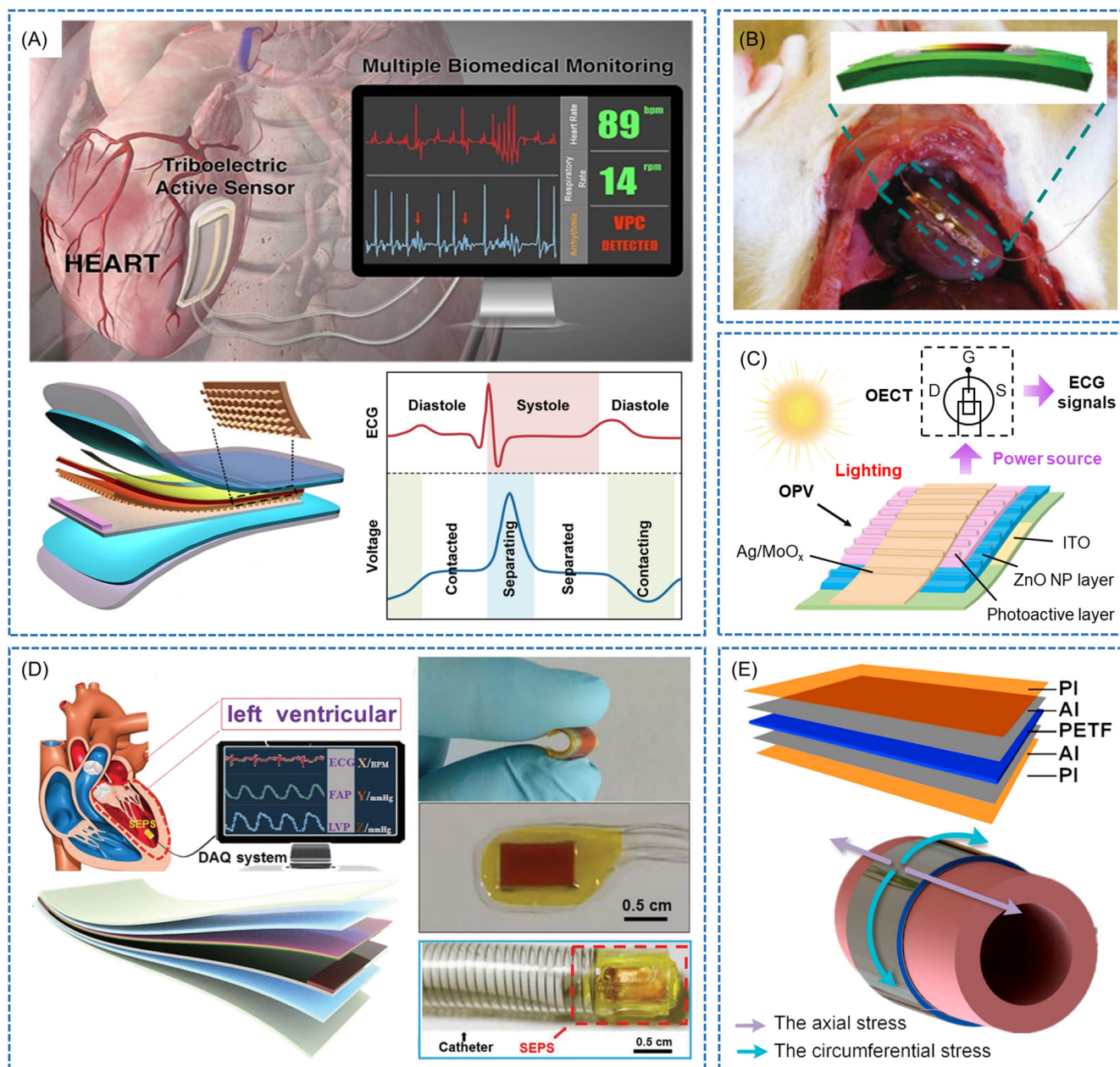


**FIGURE 7** A, TENG<sup>71</sup> and B, PENG<sup>63</sup> as implantable self-powered cardiac sensors. Reproduced with permission.<sup>71</sup> Copyright 2016, American Chemical Society. Reproduced with permission.<sup>63</sup> Copyright 2010, John Wiley & Sons. C, Solar cell as power sources for implantable self-powered cardiac sensors.<sup>27</sup> D, TENG as an implantable self-powered endocardial pressure sensor. Reproduced with permission.<sup>78</sup> Copyright 2018, John Wiley & Sons. E, PENG as an implantable self-powered blood pressure sensor. Reproduced with permission.<sup>79</sup> Copyright 2016, Elsevier Publishing Group

In 2010, Li et al fabricated a flexible PENG-based energy harvester using a two-ends-bonded ZnO nanowire (NW) (Figure 7B).<sup>63</sup> ZnO NWs have been demonstrated to show good biocompatibility and biosafety when applied in biological applications at normal concentration range.<sup>85</sup> When the ZnO NWs based PENG was tightly attached on the surface of a rat heart, it can be stretched and released periodically during the process of heart expansion and contraction. The generated electrical output signals (open-circuit voltage of 3 mV and a short-

circuit current of 30 pA on average) were almost synchronized with heart beat, which enabled the ZnO NWs based PENG to monitor heart rate in real-time. Moreover, in 2017, Kim et al fabricated a flexible thin film-based PENG with larger size (2 cm × 3 cm).<sup>68</sup> The PMN-PZT-Mn (single-crystalline (1-x) Pb(Mg<sub>1/3</sub>Nb<sub>2/3</sub>)O<sub>3</sub>-(x)Pb(Zr,Ti)O<sub>3</sub> with 0.5 mol% Mn doping) thin film based PENG was proved to be biocompatible and have higher electrical output signals (17.8 V and 1.75 μA) when implanted into a porcine heart. The generated electrical signals not

only contained heart rate and cardiac oscillation information but also can be used to charge a capacitor and power other biomedical devices.

In 2018, Park et al confirmed the feasibility of using an ultra-flexible organophotovoltaic (OPV) device as a power source for self-powered cardiac signal detection system (Figure 7C).<sup>27</sup> The bulk heterojunction of this 1D double-gating-patterned OPV consisted of an organic photoactive layer and a zinc oxide electron-transporting layer. The OPV device had the ability to maintain stabilized output power under various mechanical deformation and light illumination angle. Furthermore, the OPV and the organic electrochemical transistors (OECTs) composed integrated device had the advantage of high flexibility and bio-compatibility, therefore, it can be adhered to moveable and complex three-dimensional skin and biological tissues. The ECG signals of the rat heart with an amplitude of 2.96  $\mu$ A and a SD of 25.2 nA were measured by the integrated device under an LED lighting condition (approximately  $2 \times 10^4$  lx). This OPV-based integrated device achieved an accurate, sensitive, and continuous detection of biological signals without any external power.

In clinical practice, the endocardial pressure (EP) and blood pressure (BP) are significant indicators for heart failure and hypertension. In 2019, Liu et al reported a TENG-based self-powered endocardial pressure sensor (SEPS) (Figure 7D).<sup>78</sup> The SEPS (size, 1 cm  $\times$  1.5 cm  $\times$  0.1 cm) was composed of an Au-coated nano-PTFE film and an Al foil, copolymer spacers (thickness, 500  $\mu$ m) and PDMS encapsulation layers. The as-fabricated tiny SEPS was demonstrated to be flexible, durable, and biocompatible, which can be integrated with a surgical catheter and contribute to minimizing invasive damage of implantation on heart tissue. The SEPS can convert the pressure signal induced by cardiac contraction and relaxation into electrical signals, and showed an excellent linearity ( $R^2 = 0.997$ ) and ultrasensitivity (1.195 mV/mmHg) to the applied pressure ranging from 0 to  $\approx$ 350 mmHg. When the SEPS was implanted into the heart of an adult Yorkshire pig, the generated voltage signals had a strong link with the pressure changes in left ventricle and the left atrium, which realized the accurate recording of EP in real time. Additionally, through monitoring EP inside heart chambers, life-threatening arrhythmias, such as ventricular fibrillation and ventricular premature contraction, can also be detected.

In 2016, Cheng et al designed a PENG-based BP sensor for real-time BP monitoring (Figure 7E).<sup>79</sup> The PENG-based BP sensor was fabricated with a piezoelectric thin PVDF film sandwiched by two Al thin films acted as electrodes and then encapsulated by polyimide films. During the periodical aorta expansion and retraction, the PENG wrapped around the aorta suffered circumferential and axial stresses and induced alternating voltages

continuously. When implanted the BP sensor in a male Yorkshire porcine, a favorable linearity ( $R^2 = 0.971$ ) with a sensitivity of 14.3 mV/mmHg was achieved and a maximal instantaneous power of 40 nW was produced by this device. After more than 50 000 cycles, the BP sensor can still work stably, which enabled it to realize long-term BP monitoring in vivo. This developed implantable, self-powered PENG-based BP monitoring system exhibited great potential in alarming hypertension status visually in real-time.

Table 2 summarized the various types of self-powered sensors and their applications on monitoring heartbeat and ECG. As for heartbeat monitoring, TENG, PENG and their hybrid devices are usually used for this goal. The TENG can be an individual sensor and a power source for when monitor heartbeat. The heartbeat signals obtained by sensors implanted in pigs (10 V, 14 V) are generally higher than that obtained by sensors attached on skin (0.05 V $\sim$ 3 V), because the heartbeat signals in vitro is weak. The PyNG and solar cells have not been reported yet on this application scenario due to their own specific working mechanisms. As for ECG monitoring, TENG, PyNG, and solar cells are usually used to power the ECG units. The sizes of these devices focused on an order of centimeter. The monitoring positions mainly focused on hand, finger, chest, and heart, which are closely related with heartbeat and ECG. The in vivo experiments of these studies are carried out on either small animal (eg, rats) or big animal (eg, pigs). The types of constituent materials of TENG and PENG are obviously more than that of PyNG and solar cells, which can be ascribed to their different working mechanism. The different working mechanisms and different positions of sensors limited their material selection in the same application scenario, for instance, the materials of the implantable sensors are biocompatible.

Table 3 summarized the various types of self-powered sensors and their applications on monitoring pulse and blood pressure. As for pulse monitoring, TENG, PENG, solar cell, and their hybrid devices are usually used for this goal. The TENG, PENG, and their hybrid devices are used individual sensors. The solar cells were used as power sources to provide electricity for commercial medical sensors. As for blood pressure monitoring, the TENG and PENG are used as individual sensors for this goal. The PyNG and Solar cells have not been reported yet on this application scenario. The collected signals can be voltage and current. The sizes of these devices focused on an order of centimeter. Pulse monitoring at various artery position including wrist, finger, neck, and ankle, are closely related with heartbeat. The corresponding experiments are carried out on human skin. As for blood pressure monitoring in vivo, the monitoring positions are heart, ventricle, and aorta of pigs. The types of

**TABLE 2** Summary of self-powered sensors for heartbeat and ECG monitoring

| Signal               | Heartbeat   |  |  |   | ECG   |                     |   |
|----------------------|---|--|--|---|---|---------------------|---|
| Type                 | TENG  | PENG   | Hybrid NG  | TENG  | PyNG  | Solar cells         |   |
| Function             | Sensor  | Power source   | Sensor   | Sensor  | Power source  | Power source        |   |
| Output               | 0.06 V, <sup>57</sup> 10 V, <sup>71</sup> 1.8 V, <sup>25</sup><br>3 V, <sup>69</sup> 14 V, <sup>70</sup>  | 540 V <sup>25</sup>  | 3 mV, <sup>63</sup><br>17.8 V <sup>68</sup>                | 0.15 V <sup>65</sup>  | -   | -                   | 2.96 μA <sup>27</sup>                             |
| Size/cm <sup>2</sup> | 3.2, <sup>57</sup> 3 × 2, <sup>71</sup> 1 × 1, <sup>25</sup><br>1 × 1, <sup>69</sup> 2.5 × 1 <sup>70</sup>  | 6.5 × 2 <sup>25</sup>  | 3.5 × 7 <sup>68</sup>                                      | 3.5 × 3 <sup>65</sup>                                       | 5.7 × 5.2 <sup>4</sup>                                | 40 <sup>26</sup>    | 0.04 <sup>27</sup>                                |
| Position             | Chest, <sup>57</sup> heart swine <sup>70,71</sup><br>fingers, <sup>25,69</sup> wrist <sup>69</sup>  | Hands <sup>25</sup>  | Heart rat, <sup>63</sup> porcine <sup>68</sup>             | Finger <sup>65</sup>  | Hands <sup>4</sup>                                    | Wrist <sup>26</sup> | Heart rat <sup>27</sup>                           |
| Materials            | PTFE, <sup>25,57,70,71</sup><br>acrylic, <sup>25,57</sup><br>Cu, <sup>25,57</sup> FEP, <sup>57</sup><br>Au, <sup>70,71</sup> Al, <sup>70,71</sup><br>PET, <sup>69</sup> PDMS, <sup>69</sup> | PTFE, <sup>25</sup> Cu, <sup>25</sup><br>acrylic <sup>25</sup> | ZnO NW, <sup>63</sup><br>Mn-doped<br>PMN-PZT <sup>68</sup> | PDMS, <sup>65</sup><br>PVDF, <sup>65</sup> Ag <sup>65</sup> | Al, <sup>4</sup> FEP, <sup>4</sup><br>Cu <sup>4</sup> | -                   | PBDTTT-OFT, <sup>27</sup><br>ZnO NP <sup>27</sup> |

Note: Hybrid NG represents hybrid TENG and PENG.

**TABLE 3** Summary of self-powered sensors for pulse and blood pressure monitoring

| Signal               | Pulse  |   |   |   | Blood pressure  |   |
|----------------------|--|---|---|---|---|---|
| Type                 | TENG   | PENG  | Solar cell  | Hybrid NG   | TENG  | PENG                                    |
| Function             | Sensor   | Sensor  | Power source                                      | Sensor  | Sensor  | Sensor                                  |
| Output               | 0.3 V, <sup>54</sup> 3.5 V, <sup>69</sup><br>1.52 V, <sup>72</sup><br>5 V, <sup>73</sup> 0.3 nA, <sup>58</sup>   | 12 mV, <sup>47</sup> 65 mV, <sup>80</sup><br>0.12 V, <sup>59</sup> 5 pA <sup>86</sup>                     | 0.47 μA <sup>27</sup>                             | 35 mV <sup>64</sup>   | 17.8 mV/mmHg, <sup>71</sup><br>45.7 mV/ Pa <sup>69</sup><br>1.195 mV/mmHg, <sup>78</sup>  | 14.3<br>mV/mmHg <sup>80</sup>           |
| Size/cm <sup>2</sup> | 0.8 × 0.8, <sup>54</sup> 1 × 1, <sup>69</sup><br>1 × 2, <sup>72</sup><br>1.25 × 1, <sup>73</sup> 4, <sup>58</sup>  | 1.5 × 1.5, <sup>47</sup> 5 × 5, <sup>59</sup><br>0.8 × 0.8, <sup>86</sup>                                 | 0.04 <sup>27</sup>                                | 2 × 2, <sup>64</sup>  | 3 × 2, <sup>71</sup> 1 × 1, <sup>69</sup><br>0.5 × 1, <sup>78</sup>   | -                                       |
| Position             | Wrist, <sup>54,58,69,72</sup><br>ankle, <sup>72</sup><br>finger, <sup>72</sup> neck <sup>73</sup>  | Wrist, <sup>47,59,80</sup><br>neck, <sup>47,80,86</sup>   | Fingertip <sup>27</sup>                           | Wrist <sup>64</sup>   | Heart, <sup>71</sup> left ventricle, <sup>78</sup><br>porcine<br>fingertips, <sup>69</sup> ear <sup>69</sup>                          | Aorta<br>porcine <sup>79</sup>          |
| Materials            | Cu, <sup>54,72</sup> PDMS, <sup>54,58,69</sup><br>PET, <sup>69,73</sup> ITO, <sup>69,73</sup><br>PTFE, <sup>58,69,73</sup><br>Kapton, <sup>72</sup><br>Ag, <sup>58</sup> PU, <sup>58</sup> EVA <sup>58</sup> | P(VDF-TrFE) /<br>MWCNT, <sup>47</sup><br>PZT, <sup>80,86</sup> FEP, <sup>59</sup><br>f-PTFE <sup>59</sup> | PBDTTT-OFT, <sup>27</sup><br>ZnO NP <sup>27</sup> | P(VDF-TrFE), <sup>64</sup><br>PDMS, <sup>64</sup> PU, <sup>64</sup><br>CNTs&AgNWs <sup>64</sup> | PTFE, <sup>69,71,78</sup> Al, <sup>71,78</sup><br>Au, <sup>71,78</sup><br>PET, <sup>69</sup> ITO, <sup>69</sup><br>PDMS <sup>69</sup> | PVDF, <sup>79</sup><br>Al <sup>79</sup> |

Note: Hybrid NG represents hybrid TENG and PENG.

constituent materials of TENG and PENG are obviously more than that of solar cells, which can be ascribed to their different working mechanism.

### 3.3 | Self-powered body temperature sensors

Regulating body temperature between 36.5°C and 37.5°C under different temperature circumstances is a basic demand for people to maintain normal metabolism and

physiological activities.<sup>87,88</sup> Some diseases can cause abnormal body temperature, therefore, measuring body temperature have significant meaning in evaluating physiological status and diagnosing clinical diseases. In 2015, Wang et al reported a hybridized electromagnetic-triboelectric nanogenerator that enabled several temperature sensors to work simultaneously (Figure 8A).<sup>90</sup> The hybridized nanogenerator was based on two air-flow-driven TENGs. After integrating two electromagnetic generators (EMGs) on TENGs, the hybrid device can harvest the wasted air-flow-induced vibration energy and enhance

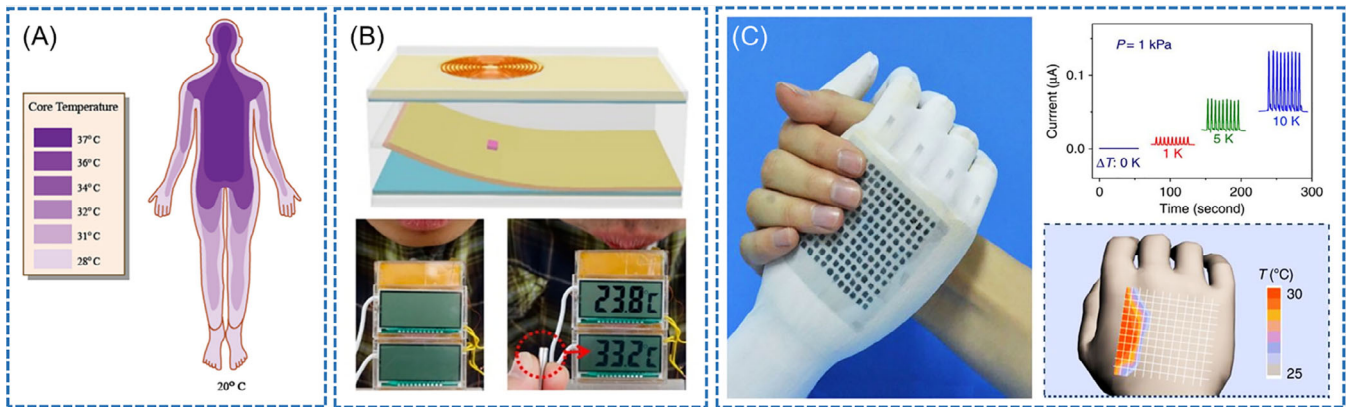


**FIGURE 8** A, Human skin temperature at ambient temperature of 20°C. Reproduced with permission.<sup>89</sup> Copyright 2012, Elsevier Publishing Group. B, TENG as a power source for self-powered body temperature sensor. Reproduced with permission.<sup>90</sup> Copyright 2015, American Chemical Society. C, TEG as a self-powered body temperature sensor. Reproduced with permission.<sup>91</sup> Copyright 2015, Springer Nature Group

the output performance of single device. Through scavenging human-mouth-blow-induced air-flow energy by this hybridized nanogenerator, two temperature sensors were powered to monitor temperatures of human fingers sustainably at the same time. Additionally, a wireless temperature monitoring system can also work well with a charged Li-ion battery by this hybridized nanogenerator.

Some researchers have demonstrated that the TENGs or PENGs made of temperature sensitive materials can serve as self-powered temperature sensors.<sup>92,93</sup> However, the resolution, accuracy, and sensitivity of TENG- and PENG-based temperature sensors are limited and not suitable for detecting body temperature due to the temperature variation ( $37 \pm 3.5^\circ\text{C}$ ) of human body.<sup>88</sup> In 2015, Zhang et al developed a high sensitive temperature sensor using thermoelectric materials, its body temperature resolution was less than 0.1 K (Figure 8B).<sup>91</sup> Meanwhile, it can also be used to detect pressure. This temperature-pressure dual-parameter sensor mainly consisted of two parts: a poly (3, 4-ethylenedioxythiophene): poly (styrenesulfonate) (PEDOT:PSS) layer served as thermoelectric material and a porous polyurethane (PU) served as microstructured frame. According to the principle of thermoelectric effect, the generated output voltage of the device presented as a function of the temperature difference between the object and the device ranging from 0.1 to 100 K. This device also exhibited an ultra-accurate temperature resolution ( $< 0.1$  K) and a fast response time ( $< 2$  seconds) to temperature difference of 1 K, which enabled it to be applicable in real-time body temperature monitoring. Additionally, during the process of temperature detecting, pressure stimuli can be quantitatively transduced into current change signals via the piezoresistive effects, the self-powered pressure-sensing sensitivity of this device was higher than  $20 \text{ kPa}^{-1}$ .

Through constructing a flexible temperature-pressure e-skin with the as-fabricated device matrixes, spatially resolved images with subtle imaging features for both temperature and pressure can be achieved.

### 3.4 | Self-powered sweat sensors

Apart from aforementioned physical signals, many kinds of biochemical signals from sweat also contain abundant medical information. By detecting and analyzing these physiological metabolic indicators, real-time health monitoring and disease diagnosis can be acquired noninvasively. Through monitoring perspiration composition such as lactate, glucose, uric acid, urea,  $\text{Na}^+$  and  $\text{K}^+$ , physiological information about tissue vitality, blood glucose, purine metabolism, gout, leukemia, and some other diseases can be achieved. In this section, some typical studies of self-powered perspiration sensors are introduced.

In 2018, He et al presented a TENG-based electronic-skin (e-skin) for real-time perspiration analysis (Figure 9A).<sup>94</sup> This e-skin was based on a polyaniline (PANI) triboelectric-biosensing unit matrix, which can convert human motion energy into electric energy. There are six biosensing unit functionalized with different enzymes on its surface, due to different enzymatic-reaction, the output currents of each biosensing unit was related closely with the concentrations of biomarkers. This e-skin can detect six physiology biomarkers of sweat separately, including lactate, glucose, urea, uric acid,  $\text{Na}^+$ , and  $\text{K}^+$ . When attaching the e-skin on human skin, it can analyze perspiration actively and be driven by the elbow bending. Additionally, after integrating this e-skin with a visualization system,  $\text{K}^+$  concentration in sweat can also be visually identified.

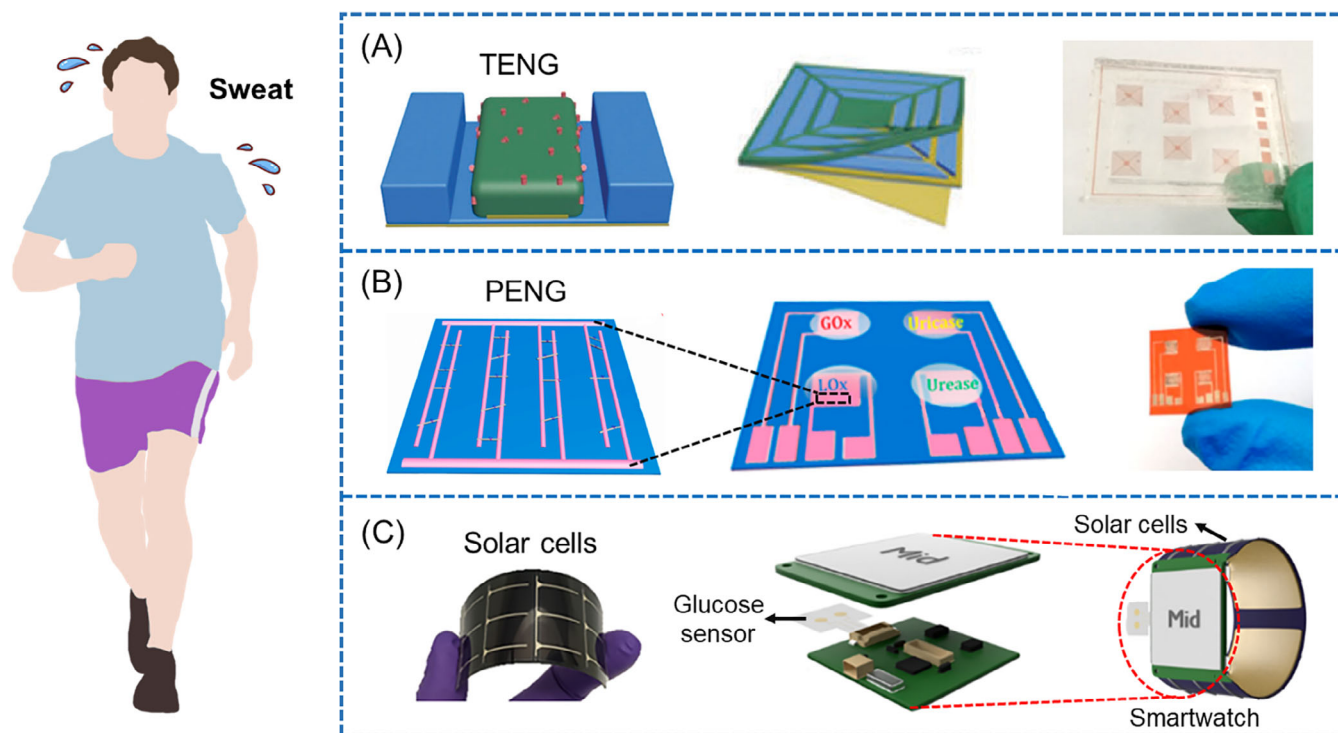


**FIGURE 9** A, TENG<sup>94</sup> and B, PENG<sup>95</sup> as self-powered perspiration sensors. Reproduced with permission.<sup>94</sup> Copyright 2018, Royal Society of Chemistry. Reproduced with permission.<sup>95</sup> Copyright 2017, American Chemical Society. C, Solar cells as a power source for self-powered perspiration sensors.<sup>96</sup> Copyright 2019, American Chemical Society

In addition to the triboelectric electronic device, the piezoelectric can be also a candidate for sweat detection. In 2017, Han et al reported a PENG-based perspiration analyzer whose core component was a piezo-biosensing e-skin with four units aligned on the substrate (Figure 9B).<sup>95</sup> The piezo-biosensing units were made of ZnO nanowire nanoarrays modified by four different kinds of enzymes including LOx (lactate oxidase), GOx (glucose oxidase), uricase, and urease on surface. The working mechanism can be ascribed to the piezoelectric-enzymatic-reaction coupling effect of enzyme/ZnO nanowires. This PENG-based perspiration sensor can be driven by strain induced by body movements and generate piezoelectric voltage signals. The output piezo-biosensing performance of the four units were dependent on the analyte concentration in the perspiration. After attached it on the forehead of a running subject, the concentration of the four biomarkers (lactate, glucose, uric acid, and urea) in the perspiration monitor can be monitored continuously in real time. The physiological state of the subject during running can be monitored by this PENG-based perspiration analyzer. Besides serving as sweat sensors, the ZnO-nanowires-based PENGs modified by GOx, uricase and urease also had ability to detect the glucose, urea and uric-acid level in body fluids of the rabbit and mouse.<sup>97-99</sup>

In 2019, Zhao et al realized real-time and continuous monitoring of sweat glucose levels by an integrated smartwatch powered by flexible photovoltaic cells (Figure 9C).<sup>96</sup> The integrated smartwatch consisted of a fully integrate system including two flexible photovoltaic cells, flexible Zn-MnO<sub>2</sub> rechargeable batteries, a sweat glucose sensor, a printed circuit board and electronic ink. The flexible photovoltaic cells can convert the outdoor sunlight energy or room light energy into electrical energy. The obtained energy can be stored in the Zn-MnO<sub>2</sub> rechargeable batteries and contributed to supporting the sensing, signal processing, and data display units continuously. For this integrated power supply module, it took less than 1 hour to charge it to 6.0 V under outdoor sunlight, the stored solar energy can support system functions for around 8 hours in dark; if under room light illumination, it can be charged to 4.2 V through about 2 hours room, and keep the whole system workable for 1 hour. The sweat glucose sensor exhibited an average sensitivity of 3.18 nA  $\mu\text{M}^{-1}$  during the 2 hours long-term measurement, according to the output currents of the sensors, the glucose concentration in sweat can be evaluated and the display of the smartwatch can provide alarm signals from “low” (< 40  $\mu\text{M}$ ), “medium” (40  $\mu\text{M}$ –120  $\mu\text{M}$ ), to “high” (> 120  $\mu\text{M}$ ). This as-fabricated self-powered smartwatch was demonstrated to

**TABLE 4** Summary of self-powered sensors for molecule monitoring

| Type Function        | TENG Sensor  | PENG Sensor   | Solar Power source                       |
|----------------------|--|---|--|
| Molecule             | Sweat (urea, uric acid, lactate, glucose, Na <sup>+</sup> , and K <sup>+</sup> ) <sup>94</sup> | Sweat (lactate, glucose, uric acid, and urea), <sup>95</sup> body fluid (glucose), <sup>97</sup> blood (glucose), <sup>98</sup> body fluid (urea/uric-acid) <sup>99</sup> | Sweat (glucose) <sup>96</sup>            |
| Size/cm <sup>2</sup> | 5 × 10 <sup>94</sup>   | 1.4 × 1.5, <sup>95</sup> 0.6 × 0.6, <sup>97</sup> 0.4, <sup>98</sup> 1 <sup>99</sup>  | -  |
| Position             | Arm <sup>94</sup>  | Wrist, <sup>95</sup> forehead, <sup>97</sup> mouse <sup>98,99</sup>   | Wrist <sup>96</sup>                      |
| Materials            | PDMS, <sup>94</sup> PANI, <sup>94</sup> Cu <sup>94</sup>                                       | ZnO NW <sup>95,97-99</sup>  | Silicon photovoltaic cells <sup>96</sup> |

realize daily visual glucose level monitoring and fitness management.

Table 4 summarized the various types of self-powered sensors and their applications on monitoring molecules. The TENG and PENG can be used as individual sensors. The solar cells are used as power sources for commercial sensors. Compared with the commercial sensors, the TENG- and PENG-based sensors consist of few sensing units modified by different kinds of enzymes can detect various molecules at the same time. The monitored molecules mainly come from the sweat, blood, and body fluid, which contains plenty of molecules related to human health. The sizes of these devices focused on an order of centimeter. When monitoring sweat, the monitoring position mainly focus on arm, wrist, and forehead. When monitoring blood and body fluid, the experiments can be carried out on mouse. The amount of material type of these sensors are similar due the limited research reports in this direction.

### 3.5 | Other medical signals detected by energy harvesters based sensing systems

In addition to aforementioned medical information related to respiration, cardiovascular system, body temperature, and perspiration, the self-powered sensors based on or powered by energy harvesters were also demonstrated to show capacity in detecting other medical signals deriving from bladder,<sup>100</sup> eye ball,<sup>101</sup> stomach,<sup>31</sup> and brain.<sup>102</sup>

In 2018, Hassani et al realized the fullness status detection of bladder by a sponge-based TENG (Figure 10A).<sup>100</sup> This TENG-based bladder sensor consisted of a thin 50 μm-thick PET layer and a flexible PVC layer with the same size. Two Cu electrode layers were attached on the bottom of PET layer and top of the PVC layer. A PDMS layer and a 1 mm-thick wet sponge layer were placed between the two Cu electrodes. Due to the

triboelectrification and electrostatic induction between the PDMS layer, water and Cu electrodes, the output voltage of the bladder sensor increased from 35.6 mV to 114 mV when the applied force increased from 0 to 6.86 N. Therefore, the filling and voiding of the rat bladder can result in the changes of output voltage. Additionally, this TENG-based bladder sensor can be integrated with a shape-memory-alloy-based bistable actuator, which enabled the filling status information of the rat bladder to be obtained in real time, and the bistable actuator can be activated by external voltage and empty the bladder. This integrated system can be developed into a self-control system and realize autonomous micturition in the future.

In 2014, Lee et al fabricated a super-flexible and ultrathin PENG with a total thickness of about 16 μm for eye movement tracking (Figure 10B).<sup>101</sup> The PENG was fabricated by anodizing an ultrathin Al foil, and growing ZnO nanowire (NW) film on the surface of the formed anodic aluminum oxide (AAO) layers. The insulating AAO layers had the capacity to block the electron transportation between the Al electrode and the ZnO NW film, which contributed to a high potential barrier at the interface and protects the PENG from short circuiting. The PENG-based sensor can output voltages and currents when it was compressive or tensile strained. When attaching a PENG with the active area of 3 mm × 10 mm on right eyelid, it can convert the signal of eye ball movement into electrical signals, which can be used to track eye ball movement and distinguish the rapid and slow eye movement. This self-powered PENG-based sensor had potential in monitoring sleep pattern, tiredness, and possible brain activity.

In 2017, Dagdeviren et al proposed a flexible PENG-based gastrointestinal (GI) sensor (Figure 10C).<sup>31</sup> The PENG was composed of 12 groups of lead zirconate titanate (PZT) ribbons connected in series, and there were 10 PZT ribbons connected in parallel in each group. To fully isolate the PZT-based PENG from the GI

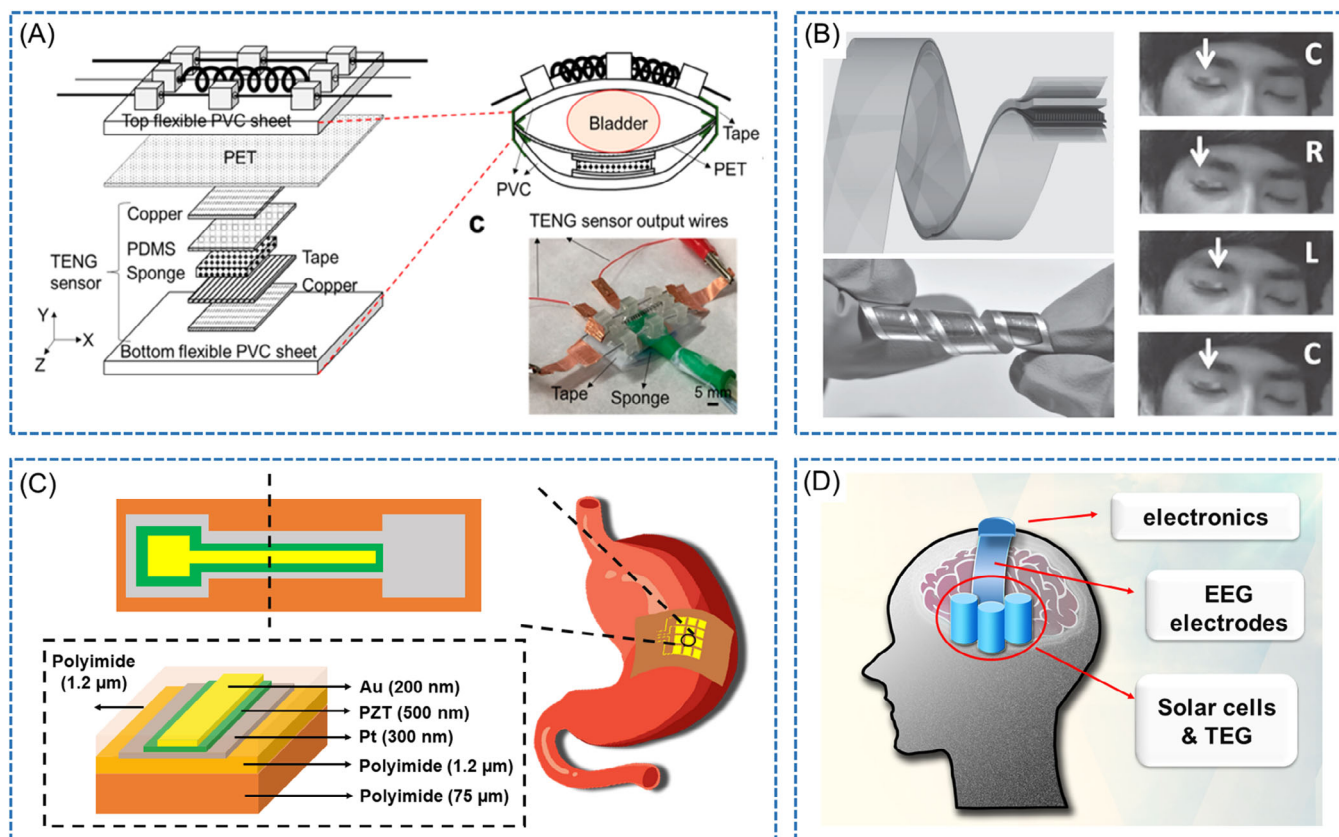


**FIGURE 10** A, Self-powered bladder sensor based on TENG. Reproduced with permission.<sup>100</sup> Copyright 2018, American Chemical Society. B, Self-powered eye ball motion sensor based on PENG. Reproduced with permission.<sup>101</sup> Copyright 2013, John Wiley & Sons C, Self-powered gastrointestinal motility based on PENG.<sup>31</sup> D, Self-powered electro-encephalography (EEG) system powered by TEGs and solar cells<sup>102</sup>

environment, it should be encapsulated by a 1.2- $\mu\text{m}$ -thick layer of poly amic acid solution and a 10- $\mu\text{m}$ -thick layer of ultraviolet curable epoxy at the outer surface. The as-fabricated PZT GI sensor was demonstrated to be mechanically and electrically stable in simulated gastric fluid and simulated intestinal fluid over 48 hours. Furthermore, this device was biocompatible, which can avoid inducing potential immunogenic reactions in vivo. To implant the device into the gastric cavity of a Yorkshire swine model noninvasive, the flexible sensor with the size of 75  $\mu\text{m}$   $\times$  2.5 cm  $\times$  2 cm was folded into an ingestible, dissolvable capsule that can be dissolved in the GI fluid, the device can unfold naturally and intimately attach onto the gastric mucosa. The air or water inflation and deflation in stomach can induce pressure change applied on the GI sensor, which resulted in the change of output voltage. The PENG-based device was capable of sensing key behaviors such as food ingestion in simulated gastric models in vitro and ex vivo. The implanted GI sensor can also be used to harvest motion energy during abdominal palpation and simultaneously generate electrical power. This PENG-based device

realized sensing safely mechanical variations and harvesting mechanical energy inside the gastrointestinal, and showed potential in diagnosing and treating motility disorders together with monitoring ingestion in bariatric applications.

EEG is a diagnostic test recording the electrical activity of the brain and has clinical applications such as epilepsy or sleep monitoring. In 2008, Torfs et al realized a self-powered, wireless and wearable electroencephalography (EEG) system powered by a hybrid device of TEGs and optional solar cells (Figure 10D).<sup>102</sup> The headphone-like TEGs produced a voltage of approx 1.5 mW at normal room temperature (22°C-23°C). However, there was almost no power generated when the outside ambient temperature approached to body temperature, because the temperature difference was too small. Through mounting the solar cells onto the radiators of the TEGs, a complementary power can be provided under indoor light (0.2 mW) and direct sunlight (45 mW). The harvested energy deriving from body heat and light can be stored in a capacitor that can provide a stable supply voltage for the EEG system. By the method, the high-

quality EEG signals can be continuously recorded and transmitted wirelessly.

## 4 | SUMMARY AND PERSPECTIVE

This review summarized the research progress of the SMIS and their applications in medical information acquisition. According to different working mechanisms, these SMIS were clarified into TENGs, PENGs, PyNGs/TEGs, solar cells, and their hybrid devices. On the basis of different medical signals, we have discussed corresponding SMIS upon their fabrication techniques, materials selections, structure designs, output performance, application scenarios, and detected medical information. For these newly invented SMIS, it still has no uniform standards or rules to evaluate their advantages and disadvantages. Therefore, it is urgently to construct a complete evaluation standard to quantitatively and qualitatively assess their performance as well as the application potential and commercial values.

### 4.1 | Function of SMIS

Due to acting different roles in sensing systems, the TENG, PENG, and PyNG/TEG themselves can work as individual active sensors and directly convert physiological signal into medical signal. On the other hand, they can also act as an independent power source of the whole sensing system to provide electricity for commercial sensors. Additionally, in some sensing systems, they can act as both active sensors and energy suppliers. Sometimes, to enhance the energy-harvesting efficiency, hybrid SMIS such as tribo-piezoelectric hybrid NG<sup>64</sup> and tribo-piezopyroelectric hybrid NG<sup>65</sup> are adopted to achieve signal detection. For the solar cells, they are mainly applied as power source in sensing system because their energy sources are limited to sunlight or environmental light, not come from body activity or body temperature. In future, the combination of multiple devices will be a development tendency. By the combination, even the weak physiological activity can be detected. The energy harvesting ability will be greatly improved.

### 4.2 | In vitro application scenarios

Depending on the monitoring positions, the acquired medical information can come from the head, forehead, eyelid, mouth, chest, wrist, and hand. The corresponding medical signals vary from EEG, sweat, eye-ball movement, respiratory rhythm, breathing component, heart

rate, pulse to body temperature. The obtained medical information provides an effective reference and guidance for doctors to further diagnose patients. These SMIS are usually wearable, flexible, or stretchable. Considering the plenty of physical activity and continuous motions in practical application, the robustness of structure, mechanical, and electric stability are the main challenge of in vitro SMIS. Additionally, the comfort and aesthetic degree should be further improved to make these sensors more acceptable and popular.

### 4.3 | In vivo application scenarios

Depending on the monitoring positions, the acquired medical information can come from various internal organs, such as aorta, stomach, heart surface, and pericardial sac. By monitoring these positions, the medical signals about ECG, heart rate, endocardial pressure (EP) and blood pressure (BP) arrhythmias, food ingestion can be obtained. These medical information reflect the health status of patients and provide timely cues for cardiovascular disease, including ventricular fibrillation, ventricular premature contraction, hypertension status and obesity, respectively. These self-powered sensors are usually implantable and biocompatible. Most of the studies related to implantable SMIS have carried out biocompatibility test and immunohistochemistry analysis by cell culture and hematoxylin and eosin (H&E) stain of surrounding tissues at the implantation site. Few reports have mentioned about the effect of implantable SMIS on the functions of organs or immunity against the diseases, which should be further studied to provide reference value for practical clinical application. Compared with in vitro environment, the in vivo scenarios are complex and susceptible to surrounding tissues. The biosafety, antijamming capability, microminiaturization are the main challenges of in vivo sensors. To make the sensors work stably for a long time in a narrow space, the sensors should be effectively fixed and miniaturized. Additionally, along with the advent of new techniques and equipment, the detected medical signals by self-powered sensors will be more diverse and comprehensive.

### 4.4 | Lifetime of SMIS

In the ideal case, the SMIS have unlimited lifetime. However, the lifetime of SMIS can be restricted by different factors in practical application. For the TENGs used in air, the common limiting factors of the lifetime came from device structure, mechanical strength of component materials, surface wear of tribo-layers, weak connection

between leading wire and back electrodes, and moisture in ambient environment. These limitations can be further optimized by stability design, diversified selection of new flexible tribo-materials, strong binding agent, and preset test environment. For the PENGs used in air, the common limiting factors of the lifetime mainly came from device structure and mechanical strength of component materials. As for the PENGs used in watery environment, if the materials are soluble in water, the device should be encapsulated by waterproof polymer film or waterproof coating. Additionally, when the TENGs and PENGs were implanted in animal body, the devices will be subjected to a long-term wrapping by surrounding tissues, which will affect the structure stability of TENGs and PENGs and then shorten their lifetime. Currently, the common used strategy is external encapsulation by waterproof polymer film or depositing waterproof coating.<sup>103,104</sup> For some specific application scenarios, a tunable lifetime of the sensor is expected. Biodegradable materials were selected for TENG or PENG fabrication.<sup>105-108</sup> The inherent biodegradability or artificially modified biodegradable property were usually obtained for component materials. For the PyNGs and solar cells, current studies showed that their lifetime ranged from several years to decades.<sup>109</sup> Compared with the lifetime, the energy conversion efficiency is the research focus. New materials or optimized structures and components will be an important research direction in future.

#### 4.5 | Signal processing of SMIS

In practical test, the signals were collected by a complete signal acquisition system, including signal generation from body, signal acquisition by wearable sensor and signal processing by auxiliary signal management modules. When the detected signal is much higher than noise, the wearable sensor has a good signal-to-noise ratio and do not rely on an external signal management module. When the magnitude of noise interferes is comparable to the detected signals, the wearable sensor relies on an external signal management module to obtain an enhanced signal-to-noise ratio. The common used signal processing instruments include low-noise current and voltage amplifiers/preamplifiers, digital filters, oscilloscopes, and signal management modules of wireless signal transmission systems. Additionally, the encapsulation of sensors is also a commonly used method to ensure the isolation from interference from the ambient environment.

Finally, considering the practical situation in clinic, an effective and precise acquisition of medical signal always needs a complete sensing system, which involves the energy conversion, power management, signal processing, signal transmitting and receiving. This expected goal relies on the multidisciplinary studies, not just the single study

of TENGs, PENGs, PyNGs/TEGs, solar cells, and other energy-harvesting devices. In our opinions, the integration of multiple functional units will be the mainstream direction for SMIS. We hope this review can provide a valid reference for future study and design of self-powered medical sensors.

#### ACKNOWLEDGMENTS

The authors thank the support of National Key R&D Project from Minister of Science and Technology, China (2016YFA0202703), National Nature Science Foundation of China (Nos. 61875015, 31571006, 81601629, and 21801019), and the National Youth Talent Support Program.

#### CONFLICT OF INTEREST

The authors declare no potential conflict of interest.

#### ORCID

Zhou Li  <https://orcid.org/0000-0002-9952-7296>

#### REFERENCES

1. Adami H-O, Day N, Trichopoulos D, Willett W. Primary and secondary prevention in the reduction of cancer morbidity and mortality. *Eur J Cancer*. 2001;37:118-127.
2. Rassi A, Dias JCP, Marin-Neto JA. Challenges and opportunities for primary, secondary, and tertiary prevention of Chagas' disease. *Heart*. 2009;95(7):524-534.
3. Park SY, Kim Y, Kim T, Eom TH, Kim SY, Jang HW. Chemoresistive materials for electronic nose: Progress, perspectives, and challenges. *InfoMat*. 2019;1:289-316.
4. Niu S, Wang X, Yi F, Zhou YS, Wang ZL. A universal self-charging system driven by random biomechanical energy for sustainable operation of mobile electronics. *Nat Commun*. 2015;6:8975.
5. Liang Y, Zhao CZ, Yuan H, et al. A review of rechargeable batteries for portable electronic devices. *InfoMat*. 2019;1(1):6-32.
6. Wu W, Haick H. Materials and wearable devices for autonomous monitoring of physiological markers. *Adv Mater*. 2018;30(41):1705024.
7. Huynh TP, Haick H. Autonomous flexible sensors for health monitoring. *Adv Mater*. 2018;30(50):1802337.
8. Hinchet R, Yoon H-J, Ryu H, et al. Transcutaneous ultrasound energy harvesting using capacitive triboelectric technology. *Science*. 2019;365(6542):491-494.
9. Khandelwal G, Chandrasekhar A, Maria Joseph Raj NP, Kim SJ. Metal-organic framework: a novel material for triboelectric nanogenerator-based self-powered sensors and systems. *Adv Energy Mater*. 2019;9(14):1803581.
10. Han M, Wang H, Yang Y, et al. Three-dimensional piezoelectric polymer microsystems for vibrational energy harvesting, robotic interfaces and biomedical implants. *Nature Electr*. 2019;2(1):26-35.
11. Zheng Q, Shi B, Li Z, Wang ZL. Recent progress on piezoelectric and triboelectric energy harvesters in biomedical systems. *Adv Sci*. 2017;4(7):1700029.
12. Ouyang H, Li Z. The first technology can compete with piezoelectricity to harvest ultrasound energy for powering medical implants. *Sci Bull*. 2019;64(21):1565-1566.

13. Lee EJ, Kim TY, Kim S-W, Jeong S, Choi Y, Lee SY. High-performance piezoelectric nanogenerators based on chemically-reinforced composites. *Energ Environ Sci*. 2018;11(6):1425-1430.
14. Shi Y, Wang Y, Deng Y, et al. A novel self-powered wireless temperature sensor based on thermoelectric generators. *Energ Convers Manage*. 2014;80:110-116.
15. Fan FR, Tian ZQ, Wang ZL. Flexible triboelectric generator. *Nano Energy*. 2012;1(2):328-334.
16. Zhao L, Zheng Q, Ouyang H, et al. A size-unlimited surface microstructure modification method for achieving high performance triboelectric nanogenerator. *Nano Energy*. 2016;28:172-178.
17. Chandrasekhar A, Vivekananthan V, Khandelwal G, Kim S-J. Sustainable human-machine interactive triboelectric nanogenerator toward a smart computer mouse. *ACS Sustain Chem Eng*. 2019;7(7):7177-7182.
18. Wen X, Wu W, Pan C, Hu Y, Yang Q, Wang ZL. Development and progress in piezotronics. *Nano Energy*. 2015;14:276-295.
19. Uchida K, Takahashi S, Harii K, et al. Observation of the spin Seebeck effect. *Nature*. 2008;455:778.
20. Kim CS, Lee GS, Choi H, et al. Structural design of a flexible thermoelectric power generator for wearable applications. *Appl Energ*. 2018;214:131-138.
21. Vazquez-Mena O, Bosco JP, Ergen O, et al. Performance enhancement of a graphene-zinc phosphide solar cell using the electric field-effect. *Nano Lett*. 2014;14(8):4280-4285.
22. Chang TH, Kung CW, Chen HW, et al. Planar heterojunction perovskite solar cells incorporating metal-organic framework nanocrystals. *Adv Mater*. 2015;27(44):7229-7235.
23. Tian B, Zheng X, Kempa TJ, et al. Coaxial silicon nanowires as solar cells and nanoelectronic power sources. *Nature*. 2007;449(7164):885.
24. Wang M, Zhang J, Tang Y, et al. Air-flow-driven triboelectric nanogenerators for self-powered real-time respiratory monitoring. *ACS Nano*. 2018;12(6):6156-6162.
25. Lin Z, Chen J, Li X, et al. Triboelectric nanogenerator enabled body sensor network for self-powered human heart-rate monitoring. *ACS Nano*. 2017;11(9):8830-8837.
26. Kim CS, Yang HM, Lee J, et al. Self-powered wearable electrocardiography using a wearable thermoelectric power generator. *ACS Energy Lett*. 2018;3(3):501-507.
27. Park S, Heo SW, Lee W, et al. Self-powered ultra-flexible electronics via nano-grating-patterned organic photovoltaics. *Nature*. 2018;561(7724):516.
28. Wang J, He T, Lee C. Development of neural interfaces and energy harvesters towards self-powered implantable systems for healthcare monitoring and rehabilitation purposes. *Nano Energy*. 2019;65:104039.
29. Wang Y, Wang HL, Li HY, Wei XY, Wang ZL, Zhu G. Enhanced high-resolution triboelectrification-induced electroluminescence for self-powered visualized interactive sensing. *ACS Appl Mater Inter*. 2019;11(14):13796-13802.
30. Ouyang H, Liu Z, Li N, et al. Symbiotic cardiac pacemaker. *Nat Commun*. 2019;10(1):1821.
31. Dagdeviren C, Javid F, Joe P, et al. Flexible piezoelectric devices for gastrointestinal motility sensing. *Nat Biomed Eng*. 2017;1(10):807.
32. Wang ZL, Chen J, Lin L. Progress in triboelectric nanogenerators as a new energy technology and self-powered sensors. *Energ Environ Sci*. 2015;8(8):2250-2282.
33. Wang ZL. Triboelectric nanogenerators as new energy technology for self-powered systems and as active mechanical and chemical sensors. *ACS Nano*. 2013;7(11):9533-9557.
34. Fan FR, Lin L, Zhu G, Wu W, Zhang R, Wang ZL. Transparent triboelectric nanogenerators and self-powered pressure sensors based on micropatterned plastic films. *Nano Lett*. 2012;12(6):3109-3114.
35. Zhu G, Pan C, Guo W, et al. Triboelectric-generator-driven pulse electrodeposition for micropatterning. *Nano Lett*. 2012;12(9):4960-4965.
36. Wang S, Lin L, Wang ZL. Nanoscale triboelectric-effect-enabled energy conversion for sustainably powering portable electronics. *Nano Lett*. 2012;12(12):6339-6346.
37. Wang S, Lin L, Xie Y, Jing Q, Niu S, Wang ZL. Sliding-triboelectric nanogenerators based on in-plane charge-separation mechanism. *Nano Lett*. 2013;13(5):2226-2233.
38. Zhu G, Chen J, Liu Y, et al. Linear-grating triboelectric generator based on sliding electrification. *Nano Lett*. 2013;13(5):2282-2289.
39. Zhu G, Chen J, Zhang T, Jing Q, Wang ZL. Radial-arrayed rotary electrification for high performance triboelectric generator. *Nat Commun*. 2014;5:3426.
40. Su Y, Zhu G, Yang W, et al. Triboelectric sensor for self-powered tracking of object motion inside tubing. *ACS Nano*. 2014;8(4):3843-3850.
41. Niu S, Liu Y, Wang S, et al. Theoretical investigation and structural optimization of single-electrode triboelectric nanogenerators. *Adv Funct Mater*. 2014;24(22):3332-3340.
42. Wang S, Niu S, Yang J, Lin L, Wang ZL. Quantitative measurements of vibration amplitude using a contact-mode free-standing triboelectric nanogenerator. *ACS Nano*. 2014;8(12):12004-12013.
43. Niu S, Wang S, Liu Y, et al. A theoretical study of grating structured triboelectric nanogenerators. *Energ Environ Sci*. 2014;7(7):2339-2349.
44. Gao Z, Zhou J, Gu Y, et al. Effects of piezoelectric potential on the transport characteristics of metal-ZnO nanowire-metal field effect transistor. *J Appl Phys*. 2009;105(11):113707.
45. Wang ZL, Yang R, Zhou J, et al. Lateral nanowire/nanobelt based nanogenerators, piezotronics and piezo-phototronics. *Mat Sci Eng R*. 2010;70(3-6):320-329.
46. Yang R, Qin Y, Dai L, Wang ZL. Power generation with laterally packaged piezoelectric fine wires. *Nat Nanotechnol*. 2008;4(1):34.
47. Wang A, Hu M, Zhou L, Qiang X. Self-powered wearable pressure sensors with enhanced piezoelectric properties of aligned P (VDF-TrFE)/MWCNT composites for monitoring human physiological and muscle motion signs. *Nanomaterials*. 2018;8(12):1021.
48. Xue H, Yang Q, Wang D, et al. A wearable pyroelectric nanogenerator and self-powered breathing sensor. *Nano Energy*. 2017;38:147-154.
49. Wen Z, Chen J, Yeh M-H, et al. Blow-driven triboelectric nanogenerator as an active alcohol breath analyzer. *Nano Energy*. 2015;16:38-46.
50. Fu Y, He H, Zhao T, et al. A self-powered breath analyzer based on PANI/PVDF piezo-gas-sensing arrays for potential diagnostics application. *Nano-Micro Lett*. 2018;10(4):76.

51. Zhang Q, Liang Q, Zhang Z, et al. Electromagnetic shielding hybrid nanogenerator for health monitoring and protection. *Adv Funct Mater.* 2018;28(1):1703801.
52. Chen S, Wu N, Ma L, et al. Noncontact heartbeat and respiration monitoring based on a hollow microstructured self-powered pressure sensor. *ACS Appl Mater Inter.* 2018;10(4):3660-3667.
53. Cao R, Wang J, Zhao S, et al. Self-powered nanofiber-based screen-print triboelectric sensors for respiratory monitoring. *Nano Res.* 2018;11(7):3771-3779.
54. Liu Z, Zhao Z, Zeng X, Fu X, Hu Y. Expandable microsphere-based triboelectric nanogenerators as ultrasensitive pressure sensors for respiratory and pulse monitoring. *Nano Energy.* 2019;59:295-301.
55. Zheng Q, Shi B, Fan F, et al. In vivo powering of pacemaker by breathing-driven implanted triboelectric nanogenerator. *Adv Mater.* 2014;26(33):5851-5856.
56. Wang S, Tai H, Liu B, et al. A facile respiration-driven triboelectric nanogenerator for multifunctional respiratory monitoring. *Nano Energy.* 2019;58:312-321.
57. Bai P, Zhu G, Jing Q, et al. Membrane-based self-powered triboelectric sensors for pressure change detection and its uses in security surveillance and healthcare monitoring. *Adv Funct Mater.* 2014;24(37):5807-5813.
58. Chen X, Parida K, Wang J, et al. A stretchable and transparent nanocomposite nanogenerator for self-powered physiological monitoring. *ACS Appl Mater Inter.* 2017;9(48):42200-42209.
59. Wang B, Liu C, Xiao Y, et al. Ultrasensitive cellular fluorocarbon piezoelectret pressure sensor for self-powered human physiological monitoring. *Nano Energy.* 2017;32:42-49.
60. Zhong T, Zhang M, Fu Y, et al. An artificial triboelectricity-brain-behavior closed loop for intelligent olfactory substitution. *Nano Energy.* 2019;63:103884.
61. Hwang BU, Lee JH, Trung TQ, et al. Transparent stretchable self-powered patchable sensor platform with ultrasensitive recognition of human activities. *ACS Nano.* 2015;9(9):8801-8810.
62. Alluri NR, Vivekananthan V, Chandrasekhar A, Kim S-J. Adaptable piezoelectric hemispherical composite strips using a scalable groove technique for a self-powered muscle monitoring system. *Nanoscale.* 2018;10(3):907-913.
63. Li Z, Zhu G, Yang R, Wang AC, Wang ZL. Muscle-driven *in vivo* nanogenerator. *Adv Mater.* 2010;22(23):2534-2537.
64. Chen X, Song Y, Su Z, et al. Flexible fiber-based hybrid nanogenerator for biomechanical energy harvesting and physiological monitoring. *Nano Energy.* 2017;38:43-50.
65. Sun J-G, Yang T-N, Wang C-Y, Chen L-J. A flexible transparent one-structure tribo-piezo-pyroelectric hybrid energy generator based on bio-inspired silver nanowires network for biomechanical energy harvesting and physiological monitoring. *Nano Energy.* 2018;48:383-390.
66. Abubakar I, Tillmann T, Banerjee A. Global, regional, and national age-sex specific all-cause and cause-specific mortality for 240 causes of death, 1990-2013: a systematic analysis for the global burden of disease study 2013. *Lancet.* 2015;385(9963):117-171.
67. McGill HC Jr, McMahan CA, Gidding SS. Preventing heart disease in the 21st century: implications of the pathobiological determinants of atherosclerosis in youth (PDAY) study. *Circulation.* 2008;117(9):1216-1227.
68. Kim DH, Shin HJ, Lee H, et al. In vivo self-powered wireless transmission using biocompatible flexible energy harvesters. *Adv Funct Mater.* 2017;27(25):1700341.
69. Meng K, Chen J, Li X, et al. Flexible weaving constructed self-powered pressure sensor enabling continuous diagnosis of cardiovascular disease and measurement of cuffless blood pressure. *Adv Funct Mater.* 2019;29(5):1806388.
70. Zheng Q, Zhang H, Shi B, et al. In vivo self-powered wireless cardiac monitoring via implantable triboelectric nanogenerator. *ACS Nano.* 2016;10(7):6510-6518.
71. Ma Y, Zheng Q, Liu Y, et al. Self-powered, one-stop, and multifunctional implantable triboelectric active sensor for real-time biomedical monitoring. *Nano Lett.* 2016;16(10):6042-6051.
72. Ouyang H, Tian J, Sun G, et al. Self-powered pulse sensor for antidiastole of cardiovascular disease. *Adv Mater.* 2017;29(40):1703456.
73. Yang J, Chen J, Su Y, et al. Eardrum-inspired active sensors for self-powered cardiovascular system characterization and throat-attached anti-interference voice recognition. *Adv Mater.* 2015;27(8):1316-1326.
74. Lai YC, Deng J, Zhang SL, Niu S, Guo H, Wang ZL. Single-thread-based wearable and highly stretchable triboelectric nanogenerators and their applications in cloth-based self-powered human-interactive and biomedical sensing. *Adv Funct Mater.* 2017;27(1):1604462.
75. Ghosh SK, Mandal D. Bio-assembled, piezoelectric prawn shell made self-powered wearable sensor for non-invasive physiological signal monitoring. *Appl Phys Lett.* 2017;110(12):123701.
76. Ghosh SK, Mandal D. Sustainable energy generation from piezoelectric biomaterial for noninvasive physiological signal monitoring. *ACS Sustain Chem Eng.* 2017;5(10):8836-8843.
77. Wu M, Wang Y, Gao S, et al. Solution-synthesized chiral piezoelectric selenium nanowires for wearable self-powered human-integrated monitoring. *Nano Energy.* 2019;56:693-699.
78. Liu Z, Ma Y, Ouyang H, et al. Transcatheter self-powered ultrasensitive endocardial pressure sensor. *Adv Funct Mater.* 2019;29(3):1807560.
79. Cheng X, Xue X, Ma Y, et al. Implantable and self-powered blood pressure monitoring based on a piezoelectric thinfilm: simulated, *in vitro* and *in vivo* studies. *Nano Energy.* 2016;22:453-460.
80. Park DY, Joe DJ, Kim DH, et al. Self-powered real-time arterial pulse monitoring using ultrathin epidermal piezoelectric sensors. *Adv Mater.* 2017;29(37):1702308.
81. Hsieh H-H, Hsu F-C, Chen Y-F. Energetically autonomous, wearable, and multifunctional sensor. *ACS Sensors.* 2018;3(1):113-120.
82. Feng H, Zhao C, Tan P, Liu R, Chen X, Li Z. Nanogenerator for biomedical applications. *Adv Healthc Mater.* 2018;7(10):1701298.
83. Sun J, Yang A, Zhao C, Liu F, Li Z. Recent progress of nanogenerators acting as biomedical sensors *in vivo*. *Sci Bull.* 2019;64(18):1336-1347.
84. Parvez Mahmud M, Huda N, Farjana SH, Asadnia M, Lang C. Recent advances in nanogenerator-driven self-powered implantable biomedical devices. *Adv Energy Mater.* 2018;8(2):1701210.

85. Li Z, Yang R, Yu M, Bai F, Li C, Wang ZL. Cellular level biocompatibility and biosafety of ZnO nanowires. *J Phys Chem C*. 2008;112(51):20114-20117.
86. Yan C, Deng W, Jin L, et al. Epidermis-inspired ultrathin 3D cellular sensor array for self-powered biomedical monitoring. *ACS Appl Mater Inter*. 2018;10(48):41070-41075.
87. Evans SS, Repasky EA, Fisher DT. Fever and the thermal regulation of immunity: the immune system feels the heat. *Nat Rev Immunol*. 2015;15(6):335.
88. Lim CL, Byrne C, Lee JKW. Human thermoregulation and measurement of body temperature in exercise and clinical settings. *Ann Acad Med Singapore*. 2008;37(4):347-353.
89. Sue C-Y, Tsai N-C. Human powered MEMS-based energy harvest devices. *Appl Energ*. 2012;93:390-403.
90. Wang X, Wang S, Yang Y, Wang ZL. Hybridized electromagnetic-triboelectric nanogenerator for scavenging air-flow energy to sustainably power temperature sensors. *ACS Nano*. 2015;9(4):4553-4562.
91. Zhang F, Zang Y, Huang D, Di C, Zhu D. Flexible and self-powered temperature-pressure dual-parameter sensors using microstructure-frame-supported organic thermoelectric materials. *Nat Commun*. 2015;6:8356.
92. Wang X, Song W-Z, You M-H, et al. Bionic single-electrode electronic skin unit based on piezoelectric nanogenerator. *ACS Nano*. 2018;12(8):8588-8596.
93. Xia K, Zhu Z, Zhang H, Xu Z. A triboelectric nanogenerator as self-powered temperature sensor based on PVDF and PTFE. *Appl Phys A*. 2018;124(8):520.
94. He H, Zeng H, Fu Y, et al. A self-powered electronic-skin for real-time perspiration analysis and application in motion state monitoring. *J Mater Chem C*. 2018;6(36):9624-9630.
95. Han W, He H, Zhang L, et al. A self-powered wearable noninvasive electronic-skin for perspiration analysis based on piezo-biosensing unit matrix of enzyme/ZnO nanoarrays. *ACS Appl Mater Inter*. 2017;9(35):29526-28537.
96. Zhao J, Lin Y, Wu J, et al. A fully integrated and self-powered smartwatch for continuous sweat glucose monitoring. *ACS Sensors*. 2019;4(7):1925-1933.
97. Xue X, Qu Z, Fu Y, Yu B, Xing L, Zhang Y. Self-powered electronic-skin for detecting glucose level in body fluid basing on piezo-enzymatic-reaction coupling process. *Nano Energy*. 2016;26:148-156.
98. Zhang W, Zhang L, Gao H, et al. Self-powered implantable skin-like glucometer for real-time detection of blood glucose level *in vivo*. *Nano-Micro Lett*. 2018;10(2):32.
99. Yang W, Han W, Gao H, et al. Self-powered implantable electronic-skin for in situ analysis of urea/uric-acid in body fluids and the potential applications in real-time kidney-disease diagnosis. *Nanoscale*. 2018;10(4):2099-2107.
100. Hassani FA, Mogan RP, Gammad GG, et al. Toward self-control systems for neurogenic underactive bladder: a triboelectric nanogenerator sensor integrated with a bistable micro-actuator. *ACS Nano*. 2018;12(4):3487-3501.
101. Lee S, Hinchet R, Lee Y, et al. Ultrathin nanogenerators as self-powered/active skin sensors for tracking eye ball motion. *Adv Funct Mater*. 2014;24(8):1163-1168.
102. Torfs T, Leonov V, Yazicioglu RF, et al. Wearable autonomous wireless electro-encephalography system fully powered by human body heat. *Sensors*. 2008 *IEEE*. 2008;1269-1272. <https://doi.org/10.1109/ICSENS.2008.4716675>
103. Chandrasekhar A, Vivekananthan V, Khandelwal G, Kim SJ. A fully packed water-proof, humidity resistant triboelectric nanogenerator for transmitting Morse code. *Nano Energy*. 2019;60:850-856.
104. Zheng Q, Jin Y, Liu Z, et al. Robust multilayered encapsulation for high-performance triboelectric nanogenerator in harsh environment. *ACS Appl Mater Inter*. 2016;8(40):26697-26703.
105. Li H, Zhao C, Wang X, et al. Fully bioabsorbable capacitor as an energy storage unit for implantable medical electronics. *Adv Sci*. 2019;6(6):1801625.
106. Li Z, Feng H, Zheng Q, et al. Photothermally tunable biodegradation of implantable triboelectric nanogenerators for tissue repairing. *Nano Energy*. 2018;54:390-399.
107. Jiang W, Li H, Liu Z, et al. Fully bioabsorbable natural-materials-based triboelectric nanogenerators. *Adv Mater*. 2018;30(32):1801895.
108. Zheng Q, Zou Y, Zhang Y, et al. Biodegradable triboelectric nanogenerator as a life-time designed implantable power source. *Sci Adv*. 2016;2(3):e1501478.
109. Amatya R, Ram RJ. Solar thermoelectric generator for micro-power applications. *J Electron Mater*. 2010;39(9):1735-1740.

## AUTHOR BIOGRAPHIES



Luming Zhao received the B.E degree in Huazhong University of Science and Technology, China in 2014. She is currently pursuing the Ph.D. degree at Beijing Institute of Nanotechnology and Nanosystem, Chinese Academy of Sciences. Her research work is focusing on nanogenerator, high sensitive sensors (e.g., UV, molecule or biosensors) and piezoelectric nanowire device.



Hu Li received the B.S. degree in School of Material Science and Engineering from Tianjin Polytechnic University in 2014. He is currently pursuing the Ph.D. degree in School of Biological Science and Medical Engineering in Beihang University. His research interests are focusing on triboelectric electronics, implantable & biodegradable electronics, energy storage and self-assembly of nanomaterials.



Jianping Meng received his Ph.D. from General Research Institute for Nonferrous Metals, China in 2017, Master's Degree from China University of Geosciences (Beijing), China in 2013, and Bachelor's Degree from Liaoning Technical University, China in 2010.

He is currently working as the Assistant Professor at Beijing Institute of Nanoenergy and Nanosystems, Chinese Academy of Science. His research interest includes nanomaterial, biosensor, and triboelectric nanogenerator.



Prof. Zhou Li is full Professor in Beijing Institute of Nanoenergy and Nanosystems, and School of Nanoscience and Technology, University of Chinese Academy of Sciences. His research interest focused on the nanogenerators, self-powered medical system, implantable energy harvesting devices, single cell mechanics and nano-biosensors. He is the Vice-Chairman of Youth Committee in the China Society of Biomedical Engineering, the Youth Committee member of the China Society of Biological

Engineering. He is selected to join the National Youth Talent Support Program, New Century Excellent Talents of Ministry of Education of China, Beijing Novo Program and Beijing Top-notch Talent Program Prof. Li have been awarded Science and Technology Award of Beijing, “Young Investigator’s Award” of International Federation for Medical and Biological Engineering (IFMBE) and Gold Award of China Association of Inventions.

**How to cite this article:** Zhao L, Li H, Meng J, Li Z. The recent advances in self-powered medical information sensors. *InfoMat*. 2020;2:212–234. <https://doi.org/10.1002/inf2.12064>